



Resilient passive cooling strategies during heat waves: A quantitative assessment in different climates

Douaa Al-Assaad^{a,b,*}, Abantika Sengupta^{a,c}, Peihang An^a, Hilde Breesch^a, Afshin Afshari^d, Deepak Amaripadath^e, Shady Attia^f, Fuad Baba^g, Vincenzo Corrado^h, Letícia Eliⁱ, Amanda F. Krelling^{i,j}, Sang Hoon Lee^j, Ronnen Levinson^j, Marcelo Olingerⁱ, Mamak P. Tootkaboni^h, Liangzhu (Leon) Wang^k, Chen Zhang^l, Michele Zinzi^m

^a KU Leuven, Department of Civil Engineering, Building Physics and Sustainable Buildings, Ghent Campus, Ghent, Belgium

^b Building Physics and Services, Eindhoven University of Technology, the Netherlands

^c Ghent University, Department of Architecture and Urban Planning, Ghent, Belgium

^d Fraunhofer Institute for Building Physics, Valley, Germany

^e School of Geographical Sciences and Urban Planning, Arizona State University, Tempe, AZ, USA

^f Sustainable Building Design Lab, Faculty of Applied Sciences, Université de Liège, Belgium

^g Faculty of Engineering, British University in Dubai, Dubai, United Arab Emirates

^h Department of Energy, Politecnico di Torino, Italy

ⁱ Laboratory for Energy Efficiency in Buildings, Federal University of Santa Catarina, Brazil

^j Building Technology and Urban Systems Division, Lawrence Berkeley National Laboratory, Berkeley, California, USA

^k Building, Civil, and Environmental Engineering, Concordia University, Canada

^l Department of the Built Environment, Aalborg University, Denmark

^m ENEA Italian National Agency for New Technologies, Energy and Sustainable Economic Development, Italy

ARTICLE INFO

Keywords:

Thermal resilience
Heat waves
Passive cooling
Quantitative assessment
Degree of shock

ABSTRACT

The frequency and severity of extreme weather events like heat waves are rising, posing significant challenges for buildings and their cooling systems. To safeguard occupants from potentially hazardous indoor temperatures, buildings and their cooling systems must be designed and managed to withstand these conditions and thus be resilient. This study assessed via building simulations the resilience performance of selected individual passive cooling strategies for five different climates (ASHRAE climate zones 2A, 3A, 3B, 4A, and 6A) and three heatwave periods (historical, future mid-term and future long-term). Resilience performance was assessed with three criteria: heatwave impact ($^{\circ}\text{C}\cdot\text{h}$ above a reference standard effective temperature), absorptivity rate ($^{\circ}\text{C}/\text{h}$), and recovery rate ($^{\circ}\text{C}/\text{h}$). Strategies such as solar shading, cool envelope materials, advanced glazing, and ventilative cooling could each reduce the heat wave impact and the absorptivity rates in all studied climates at different levels of efficiency. As the heat waves became more extreme, the performance declined at different rates depending on the climate. Some strategies were more suited to specific climates such as cool envelope materials in climate 2A. Most strategies could not speed up the recovery rates from the heat waves except for ventilative cooling in climate 3B. With careful design to maximize the benefits of favorable wind conditions, every climate could benefit from ventilative cooling strategies to speed up recovery from heat waves.

1. Introduction

Extreme heat events, or heat waves (HWs), are a growing global public health concern, worsened by climate change and urbanization. They have become more frequent, intense, and prolonged, with projections indicating further worsening under accelerated global warming

[1]. The most recent 2023 IPCC report has projected that the 1.5 $^{\circ}\text{C}$ and 2 $^{\circ}\text{C}$ thresholds are likely to be exceeded unless large-scale and immediate action is taken [2]. The impact on human health is well documented with the young and elderly particularly susceptible [3,4]. Globally, during the past 20 years, annual heat-related mortalities in people older than 65 years have nearly doubled, reaching about 300,000 deaths in 2018 [4].

* Corresponding author.

E-mail address: douaa.al-assaad@kuleuven.be (D. Al-Assaad).

<https://doi.org/10.1016/j.buildenv.2025.112698>

Received 30 October 2024; Received in revised form 29 January 2025; Accepted 8 February 2025

Available online 9 February 2025

0360-1323/© 2025 Elsevier Ltd. All rights reserved, including those for text and data mining, AI training, and similar technologies.

Nomenclature	
<i>English symbols</i>	
AWD	ambient warmth degree (-)
doS	normalized degree of shock (-)
GSI	global solar irradiance (W/m ²)
IOD	indoor overheating degree (-)
SET	standard effective temperature (°C)
SET _{alert}	alert-level standard effective temperature (°C)
SET _{emergency}	emergency level standard effective temperature (°C)
SET _{max}	maximum standard effective temperature reached during a heatwave (°C)
SET DH	degree hours above SET (°C.h)
SET DH*	normalized degree hours above SET (-)
SHGC	solar heat gain coefficient (-)
SR	solar reflectance (-)
ST	solar transmittance (-)
t	time (h)
T	temperature (°C)
TE	thermal emittance (-)
T _{db}	dry bulb temperature (°C)
T _{oa}	outdoor air temperature (°C)
T _z	zonal air temperature (°C)
TRI	thermal resilience index (-)
VT	visible transmittance (-)
WWR	window-to-wall ratio (-)
<i>Greek symbols</i>	
α	overheating escalation factor
Δ _{abs}	absorptivity rate (°C/h)
Δ _{rec}	recovery rate (°C/h)
Δ _{abs} *	normalized absorptivity rate (-)
Δ _{rec} *	normalized recovery rate (-)
ΔSET	different between maximum SET and SET _{alert}
<i>Abbreviation</i>	
HW	heat wave
IEA EBC	International Energy Agency Energy in Buildings and Communities
KPI	key performance indicator
RCP	representative concentration pathway
TMY	typical meteorological year

Even under the current climate, which can still be considered mild in comparison to future projections [5,6], monitoring campaigns have shown evidence of indoor overheating. A 2010 study conducted across 122 dwellings in London, showed that 37 % of living rooms and 49 % of bedrooms exceeded the recommended adaptive comfort zone for more than 1 % of the time during occupied summer hours [7]. In senior dwellings in different US cities, temperatures exceeded the upper safe limits for most buildings [8,9]. Similar campaigns conducted in other types of buildings and locations showed similar issues [10–13]. HWs can cause major power outages, threatening critical building services and increasing risks of overheating [14]. Thus, buildings designed according to existing standards may become obsolete in the future [15,16].

Consequently, it is essential to implement long-term resilient solutions. Resilience is a performance characteristic, defined as the extent to which a building can maintain safe and habitable conditions for occupants in response to disruptive events (e.g., HWs) [17,18]. The International Energy Agency Energy in Buildings and Communities (IEA EBC) Program's Annex 80 defines resilient cooling as "a capacity of the cooling system integrated with the building that allows it to withstand or recover from disturbances due to disruptions" [18]. Zhang et al. [19] reviewed and ranked traditional and novel cooling strategies qualitatively according to: absorptive capacity, adaptive capacity, restorative capacity and recovery speed. Absorptive capacity refers to the ability of the building to absorb disturbances such as HWs. Adaptive capacity highlights the building's ability to modify its operations in response to changing environmental conditions. Restorative capacity describes how quickly and effectively a building can return to a pre-disturbance state after an extreme event. Recovery speed evaluates how quickly the building can regain its normal thermal performance after experiencing disturbances. For instance, strategies such as solar shading were qualified as having low to moderate absorptive capacity and low adaptive capacities.

The resilience of many individual strategies qualitatively reviewed in Ref. [19] were assessed quantitatively in different climates using different key performance indicators (KPIs). Yoon et al. [20] evaluated the resilience of internal vs. external thermal mass in an office located in Cambridge, MA, USA (climate zone 5A according to ASHRAE Standard 169 [21]). They found that internal mass substantially lowered peak temperatures while external mass delayed their occurrence. Green roofs were investigated during HW periods in Barcelona, Spain (climate zone 3A) [22] and Montreal, Canada (climate zone 6A) [23] in old

constructions. The overheating escalation factor α [21] was used in Ref. [22] to assess the resilience. This KPI is determined by comparing the Indoor Overheating Degree (IOD)—a measure of how much indoor temperatures exceed comfort thresholds—with the Ambient Warmness Degree (AWD), which reflects the severity of outdoor warming conditions. A value of zero indicates no increase in overheating risk. A value between zero and one suggests a slight increase in overheating risk and a value equal or greater than one signifies a significant overheating risk with rising ambient temperatures. [22]. Results showed that green roofs in climate zone 3A had an overheating escalation factor α of 0.5 for all HW projections with better performance during shorter HWs. In [23], a thermal resilience KPI – the thermal resilience index (TRI), was introduced by the authors and is a function of the standard effective temperature (SET) [25] degree hours (SET DH). The SET is an equivalent temperature of a hypothetical or reference environment at 50 % RH where the person has the same skin temperature and wetness as the real environment. It is based on the two-node thermoregulation model of Gagge et al. [26]. Thus, the SET DH is a cumulative deviation over time from a SET threshold. It was used to evaluate the resilience of a long-term care facility against heat waves in climate zone 6A. Their results showed that among individual strategies, green roofs performed better on upper floors. Its performance was thus location-dependent showing improved resilience particularly on north and east facing facades.

Solar shading technologies were assessed in [22,23] and [26] in Houston, Texas (USA) (climate zone 2A). It was found that in climate zone 3A, α was 0.5 for all HW projections with better performance during less severe HWs. In climate zone 6A, solar shading had good performance on south and west facing façades and rooms with smaller areas. In climate zone 2A, internal window shades reduced SET DH by 8.8 % compared to a baseline with no shading. Other strategies reviewed in [19] were also tested in the literature and are summarized in Table 1.

Despite extensive literature evaluating the resilience performance of individual and combined strategies during HWs, studies were conducted within the authors' climate zones of interest. Consequently, it becomes difficult judge the resilience of multiple strategies per climate during HWs. Moreover, strategies evaluated in two or a maximum of three climates (see Table 1) did not follow uniform methodologies. Each study used a different set of KPIs assessing different resilience criteria or applied different HW prediction algorithms, hindering the evaluation process.

Table 1
Overview of the resilience performance of (a) 11 individual passive cooling strategies and (b) 5 combinations in different climates.

Strategy	Properties	Baseline	Climate zone(s) [21]	Findings
a) Individual strategies				
advanced glazing	- ^a	No baseline	3A [22]	$\alpha = 0.5$ for all HWs with better performance during shorter HWs
	U = 3.73 W/m ² K, SHGC ^b = 0.057, VT ^c = 0.42	U = 4.26 W/m ² K, SHGC = 0.25, VT = 0.564	2A [26]	Building-level SET DH reduced by 27 % compared to baseline with no strategies
cool roofs	SR ^d = 0.6	SR = 0.3	2A [26]	Building-level SET DH reduced by 5.1 % compared to baseline with no strategies
	SR = 0.6 (bright white asphalt shingles)	SR = 0.1 (conventional asphalt shingles)	3C [27]	Building-level SET DH reduced by 5.4 %, 2.8 %, 2.0 % compared to baseline with no strategies for historical, future mid-term and long-term HWs
cool walls	SR = 0.6	SR = 0.3	2A [26]	Building-level SET DH reduced by 4.1 % compared to baseline with no strategies
	SR = 0.6 (off-white painted surface)	SR = 0.25 (medium-brightness colored paint)	3C [27]	Building-level SET DH reduced by 7.6 %, 6.7 %, 5.8 % compared to baseline with no strategies for historical, future mid-term and long-term HWs
ventilated cavity	Mirror finished aluminum plates, thermal emissivity of 0.8, solar absorptivity of 0.19, cavity thickness of 0.05 m	No cavity	4A [28]	Building-level SET DH reduced by 35 %, 24 %, 18 % compared to baseline for historical, future mid-term and long-term HWs
natural ventilation	3 ACH	No natural ventilation	2A [26]	Building-level SET DH reduced by 61.6 % compared to baseline with no strategies
	Window opening area of 50 %. Windows are open when the indoor temperature is higher than 26 °C and higher than the outdoor temperature	Window opening area of 10 %, user operated (schedule not specified)	6A [23]	Higher zone level TRI in upper floors and zones facing North, South and East.
night ventilation	Exhaust fans Operating time 9pm ~ 10am; Fan total efficiency 0.6; Maximum ACH of 5 Bottom hung windows open from 9 pm to 6 am in the living and sleeping rooms and on top of the stairway	No night ventilation	6A [23]	Higher zone level TRI in upper floors and zones facing North and East.
		No baseline	4A [29]	The highest operative temperature in the living room during a HW is 33°C. It took 84 h to bring temperatures below 25 °C in that room. The percentage of occupied hours above 25°C increased by 13.3 % compared to the typical meteorological year (TMY).
b) Combination of strategies				
cool roof, cool wall	roof: white asphalt shingles, walls: off-white painted surface, SR = 0.6	roof: conventional asphalt shingles), SR = 0.3 walls: medium-brightness colored paint, SR = 0.25	3C [27]	Building-level SET DH reduced by 9.8 %, 9.5 %, 8.6 % compared to baseline with no strategies for historical, future mid-term and long-term HWs
	roof: thermal absorptance 0.9, solar absorptance 0.2, walls: thermal absorptance 0.9, solar absorptance 0.4	-	4A [28]	Building-level SET DH reduced by 34 %, 26 %, 20 % compared to baseline for historical, future mid-term and long-term HWs
cool roof, cool wall, natural ventilation, air sealing, advanced glazing, solar shading	Roof & walls: SR = 0.6 Natural ventilation: 3 ACH, Air sealing: 0.25 ACH Advanced glazing: U = 3.73 W/m ² K, SHGC = 0.057, VT = 0.42 Shading: SR = 0.8	Roof & walls: SR = 0.3, No natural ventilation, Air sealing: 0.3 ACH Glazing: U = 4.26 W/m ² K, SHGC = 0.25, VT = 0.564, no shading	2A [26]	Building-level SET DH reduced by 17.1 % compared to baseline with no strategies
cool roof, cool wall, ventilated cavity	roof: thermal absorptance 0.9, solar absorptance 0.2, walls: thermal absorptance 0.9, solar absorptance 0.4 Cavity: Mirror finished aluminum plates, thermal emissivity of 0.8, solar absorptivity of 0.19, cavity thickness of 0.05 m	Roof & walls: -No cavity	4A [28]	Building-level SET DH reduced by 36 %, 25 %, 25 % compared to baseline for historical, future mid-term and long-term HWs
adiabatic cooling, night ventilation, shading	Adiabatic cooling: Operation time 7:30 am - 6:00 pm, maximum capacity of 13.1 kW, maximum flow rate 4400 m ³ /h, Night ventilation: top hung windows, operation time 10 pm - 6 am, open when the indoor temperature is higher than 23 °C and higher than the outdoor temperature by 2 °C, shading: external screens that close when solar radiation exceeds 250 W/m ² on window	No baseline	4A [30]	Zone-level DH during occupied hours increased linearly with increasing HW severity, intensity and/or duration and were orders of magnitude higher than the TMY

^a Information not provided in the paper.

^b Solar reflectance = SR.

^c Visible transmittance = VT.

^d Solar heat gain coefficient = SHGC.

The aim of this work is to evaluate the resilience performance of individual passive cooling strategies across different climate zones in representative buildings. The climates 2A, 3A, 3B, 4A and 6A, cover a wide variety of weather patterns. Moreover, this work uses the same HW prediction methods across climates [31] and the same set of resilience KPIs covering three distinct criteria of thermal resilience performance: heatwave impact, absorptivity, recovery rates. It contributes to IEA EBC's Annex 80 "Resilient cooling of Buildings" and is a companion study to the qualitative assessment of resilient cooling strategies conducted in Ref. [19]. The novelty of this paper lies in its application of a quantitative resilience assessment that incorporates simultaneously three distinct resilience performance metrics, which have not been previously used in the literature. These metrics are applied across diverse climates and reference buildings for the first time, enabling a comprehensive evaluation of passive cooling strategies' effectiveness in minimizing heat stress during extreme or prolonged HWs. This approach goes beyond traditional overheating assessments by offering a more dynamic and holistic evaluation of resilience under climate extremes.

2. Methods

The thermal resilience performance of 5 buildings across different climates was investigated under two conditions: (a) the baseline case with no strategies and (b) the case implemented with individual passive cooling strategies. This manuscript defines passive cooling as cooling methods that rely on natural processes (such as convection, radiation, or evaporation) and renewable resources without active mechanical cooling systems like compressors or extensive energy inputs. The strategies that will be considered here are cool roofs, cool walls, advanced glazing, shading and ventilative cooling (natural ventilation, adiabatic cooling). Note that despite the possibility of fan usage with adiabatic cooling and natural ventilation, they will be considered as passive cooling strategies as they rely mainly on water evaporation and convection from outdoor air respectively to reduce the air temperature. The evaluation was carried out under multiple HWs. The workflow adopted can be seen in Fig. 1. Since the focus was on assessing the performance of passive cooling strategies within each climate zone, without making cross-climate comparisons, there was no need to normalize the results based on building characteristics such as mass, volume, occupation times, fenestration extent, and surface areas facing the equator. Studies that want to compare across different climates may require normalization to account for variations in these factors.

2.1. Case study buildings

Table 2 gives an overview of the different buildings. Table 3 presents the thermal characteristics of all the cooling strategies. All the considered buildings were free running with no mechanical cooling or ventilation. The baseline cases are the buildings with no strategies. The retrofitted cases are the baseline cases implemented with the individual available cooling strategies which will be simulated for different HW scenarios. The case study buildings had to be representative cases that must comply with national building codes and standards. Further information regarding the buildings can be found in the supporting references found in Table 2 and in the e-component.

2.2. Definition and quantification of historical and future heatwave weather scenarios

The IEA EBC Annex 80 developed a methodology that defines historical and future weather files covering three time periods: historical or contemporary (2001–2020), mid-term future (2041–2060), and long-term future (2081–2100) [31,44]. There were many future climate datasets available to choose from. There are global climate models having a coarse resolution making them unsuitable for building thermal simulations and local impact studies such as resilience assessment due to

HWs [45]. An alternative was to use statistical downscaling (morphing method [46], stochastic weather generators [47]). While being a simple method with low computational power, it was not adopted in [32,45] as climate change and future extreme events were not well represented, models and scenarios used depended on the tool making difficult to assess uncertainties and it assumed that future weather patterns will be similar to present-day observations. To overcome these obstacles, dynamic downscaling (regional climate models (RCMs)) was adopted. Due to their higher spatial resolution, they allow better representation of local climate effects. RCMs also have a refined time resolution, allowing them to better represent extreme events such as heat waves [48].

To assemble future weather files, multi-year climate data projections from the Coordinated Regional Downscaling Experiment (CORDEX) were used [49]. The latter are dynamically downscaled regional climate multi-year projections from global climate models. Climate data for many weather variables (dry-bulb temperature, specific humidity, atmospheric pressure, global horizontal radiation, cloud cover and wind speed) are available in NETCDF4 format. The future projections were based on the highest baseline emissions scenario defined by the IPCC, the representative concentration pathway (RCP) 8.5 [50].

In Europe, RCMs have an unprecedented resolution of ~12 km and are part of the European CORDEX (EURO-CORDEX [51]). The resolution in the Middle East and North Africa is 25 km and 50 km for the rest of the world. Data are available at the multi-year format on different time scales: monthly, daily, every six hours and three hours, during the historical period from 1976 to 2005 and for the future period, from 2006 to 2100. Since the CORDEX data have a time step of 3 h, interpolations were made to downscale to 1 h format. Bias adjustment of the raw outputs from the RCMs was also conducted for both the historical and future periods. Subsequently, the climate data was divided into three 20-year periods (historical, future mid-term and future long-term).

After obtaining the 1-hour bias adjusted data over the historical and future periods (mid-term and long-term), future weather files could be assembled. They include typical years (TMY) defined according to the EN ISO 15,927 4:2005 [52] and extreme heatwave years according to the method of Ouzeau et al. [53]. From the temperature time series, three thresholds (S_{pic} , S_{deb} and S_{int}) could then be calculated and the heatwave years subsequently detected. S_{pic} represents the threshold beyond which a heatwave event is detected (99.5 percentile of the temperature distribution over the 30-year period). S_{deb} defines the beginning and the end of the heatwave (97.5 percentile) and S_{int} is the interruption threshold, used to merge two consecutive heatwave events without a significant drop in temperature (95 percentile). Multiple heatwave events can be detected in the three time periods. They are characterized by different intensities (maximum daily mean temperature reached during the heatwave), duration (in days) and severity (aggregated temperature above the 97.5 threshold in °C.days). From the obtained family of heatwaves in each climate, the most intense was selected in the current study for each period as can be seen in Table 4. The TMY and HW weather data files for the considered climate zones could be downloaded from the world data center for climate platform [54].

Given that HWs have multiple characteristics and there is a total of 15 HWs to be tested, it would be advantageous for visualization purposes to represent each HW with a single normalized value that combines these characteristics—specifically, its duration and intensity. For this purpose, the normalized degree of shock (doS) introduced in [30] will be adapted. The normalized doS is expressed in Eq. (1) as the product of the HW relative magnitude and duration. The relative magnitude is the ratio of the difference in the average HW dry bulb temperature ($T_{db,HW}$) and TMY dry bulb temperature during the same period of occurrence of the HW ($T_{db,TMY}$) over $T_{db,TMY}$. The relative duration is defined as the ratio of the HW duration (t_{HW}) to that of the longest possible HW ($t_{HW,longest}$) that can be detected per climate zone in the time frame in which the HWs occur. Note that for each of the three

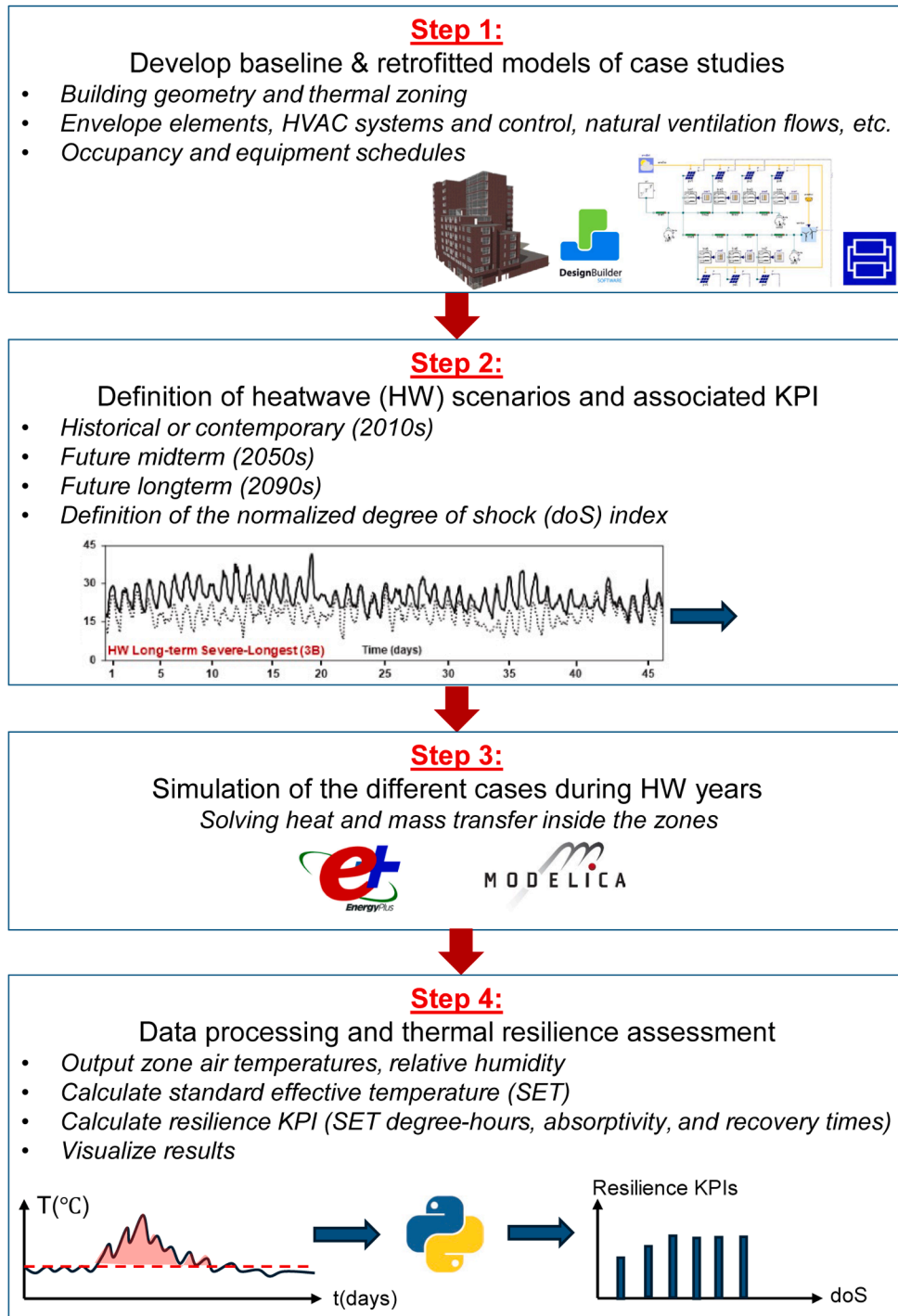


Fig. 1. Illustration of the methodology and workflow.

time periods (historical, future mid-term and long-term), there is a corresponding TMY weather file that is used to calculate $T_{db,TMY}$. Thus, the doS calculation considers the dynamic effect of global warming. Table 4 illustrates the doS for the different climate zones and the different time periods. More information can be found in the e-component.

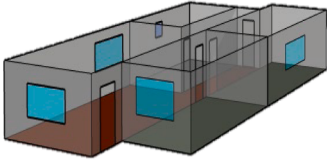
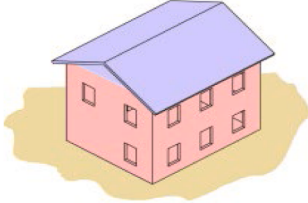
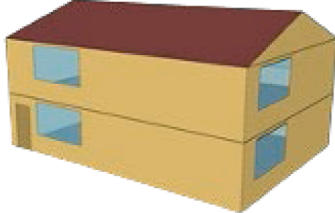
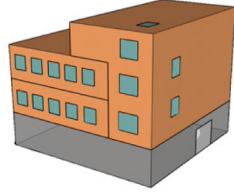
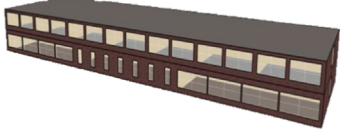
$$doS = \underbrace{\frac{T_{db,HW} - T_{db,TMY}}{T_{db,TMY}}}_{\text{Relative magnitude}} \times \underbrace{\frac{t_{HW}}{t_{HW,longest}}}_{\text{Relative duration}} \quad (1)$$

2.3. Thermal resilience assessment

The thermal resilience assessment followed the quantitative framework based on [36] which proposes to characterize the resilience performance by three aspects: a) HW impact, b) Absorptivity rate and c) Recovery rate assessed during occupied hours.

HW impact: The HW impact is expressed using the $SET DH$ [55]. It depends on the maximum SET reached (SET_{max}), the time it takes to reach it from a pre-defined temperature threshold as well as the time it takes to go back to this threshold from SET_{max} . The SET is an equivalent temperature of a hypothetical or reference environment at 50 % RH where the person has the same skin temperature and wetness as the real

Table 2
Illustration of the simulated case study buildings and corresponding cooling strategies in climate zones 2A, 3A, 3B, 4A and 6A.

City	Climate zone [21]	Building information	Building illustration	Baseline	Simulated cooling strategies
Sao Paulo, Brazil	2A	detached two-bedroom single-family home [30,31]		No mechanical cooling/ventilation. Naturally ventilated (45 % of window opening) ^a	advanced solar shading, cool roof, cool walls, advanced glazing and ventilative cooling
Rome, Italy	3A	refurbished single-family house for the construction period 1946–1960 [34]		No mechanical cooling/ventilation. Naturally ventilated	advanced solar shading, cool roof, advanced glazing and ventilative cooling
Los Angeles, CA, USA	3B	detached three-bedroom single-family home [33]		No mechanical cooling or mechanical/natural ventilation	advanced solar shading, cool roof, cool walls, advanced glazing, and ventilative cooling
Ghent, Belgium ^b	4A	two-floor educational building [30,35,36]		No mechanical cooling or mechanical/natural ventilation	advanced solar shading and ventilative cooling
Montreal, Canada	6A	two-floor educational building [40–43]		No mechanical cooling or mechanical/ natural ventilation	advanced solar shading, cool roof and ventilative cooling

^a Retrofitted case improved window opening to 100 % (Table 3).

^b Other resilient studies conducted in Belgium [37–39].

environment. It is based on the two-node thermoregulation model of Gagge et al. [56]. It can be calculated using the pythermalcomfort Python package [57]. The SET is calculated for each HW weather file generated according to the methodology of Machard et al. [32,45], for each climate zone and each of the three time periods (Table 4).

The ASHRAE 7-point predicted thermal sensation (PTS) scale can be used to quantify occupants' perceived thermal sensation within a space. It ranges from -3 (cold) to +3 (hot). Eq. (2) shows the relationship between the SET and the PTS derived in [58] for an average population. Different regression models exist for different climates and reflect the adaptability of different populations [59].

$$PTS = 0.25SET - 6.03, R^2 = 0.998 \quad (2)$$

According to Eq. (2), three SET thresholds (SET_{comf} , SET_{alert} , SET_{emer}) can be determined in relation to occupants' heat stress [60,61]. For an average population, when $PTS = 0$ (neutral), $SET_{comf} = 24.12^\circ\text{C}$; when $PTS = 1$ (slightly warm), $SET_{alert} = 28.12^\circ\text{C}$; and when $PTS = 2$ (warm), $SET_{emer} = 32.12^\circ\text{C}$. To calculate the SET_{DH} , the SET_{alert} threshold was adopted. SET_{alert} was calculated for each climate zone considered (2A, 3A, 3B, 4A, 6A) using the PTS - SET regression models of Ji et al. [59]. The resulting thresholds were 28.8°C , 30.9°C , 29.8°C , 27.1°C , and

25.7°C , respectively. To ensure a consistent basis for evaluating resilience performance across these diverse climates, an averaged threshold was adopted. The aggregated average threshold (28.46°C) closely matched the SET_{alert} for an average population. Thus, finally, to calculate the SET_{DH} , the $SET_{alert} = 28.12^\circ\text{C}$ threshold was adopted. A conceptual curve of the SET can be seen in Fig. 2. The HW impact can be seen in the hashed red area on the curve.

To calculate the SET_{DH} , for residential buildings, the reference occupant had a metabolic rate (MET) of 1 and a clothing insulation value of 0.5 clo when awake, and MET of 0.7 and a clothing insulation value of 1.38 clo when sleeping. A MET of 1.1 and a clo of 0.57 was adopted for offices and schools [62]. According to [62], overheating occurs for average age adults when the SET_{DH} exceeds $230 \pm 42^\circ\text{C}\cdot\text{h}$.

a) **Absorptivity rate:** Absorbing a HW impacts occupants throughout the transient absorption period. The rate of change of temperature has been shown in experimental literature to have a significant impact on the health and comfort of occupants. Larger temperature step changes deviating occupants even further away from their state of thermal equilibrium are perceived as more uncomfortable.

Table 3
Illustration of the thermal properties of the different cooling strategies in each climate.

Strategy	Climate 2A	3A	3B	4A	6A
Advanced solar shading	1) Overhangs , area of 51 m ² . Horizontal position covering the entire building perimeter <i>OR</i> 2) Automated Venetian external blinds installed in the living room & bedroom. Blinds close when outdoor air temperature is ≥ 26 °C	External roller blind with solar transmittance (ST) of 13 % and SR of 42 % that closes when the global solar irradiance (GSI) on the window exceeds 300 W/m ²	1) Overhangs and fins , depth of 0.5 m, horizontal overhang on south façade; vertical fin on southern side of the window, on the east and west façades, no overhangs or fins on the north façade. <i>OR</i> 2) External solar control screens , SHGC = 0.2, VT = 0.3 3) Automated Venetian external blinds , SHGC = 0.1, VT = 0.09	Automated external shading on the south façade, operated for 15 minutes when the GSI > 250 W/m ²	External roller blind with ST = 0.10 and SR = 0.35 that close when the window GSI > 250 W/m ²
Cool materials	Cool exterior wall paint and cool roof coating with SR = 0.80, thermal emittance (TE) = 0.90	Cool roof coating with a SR = 0.50, TE = 0.86	Cool exterior wall paint <i>OR</i> cool roof coating with a SR = 0.60, TE = 0.90	n/a	Cool roof coating with SR = 0.80, TE = 0.90
Advanced glazing	Multilayer glazing , SHGC = 0.32, VT = 0.24, thermal transmittance (U) = 3.6 W/m ² .K	Ultra selected double-glazed windows , SHGC = 0.30, VT = 0.64, U = 1.2 W/m ² .K	Electrochromic dynamic glazing , switching from light (SHGC = 0.50, VT = 0.75) to dark (SHGC = 0.10, VT = 0.15) when window GSI > 100 W/m ² ; U = 1.7 W/m ² .K	n/a	n/a
Ventilative cooling	Cross natural ventilation 100 % of glazing area openable. Windows open if: 1. The room is occupied. 2. Indoor dry bulb temperature $T_{db} \geq 19$ °C; 3. Indoor $T_{db} >$ outdoor T_{db}	Mechanically driven ventilative cooling using an axial fan . 200.0 l/s, pressure drop of 200 Pa, motor power of 0.2 kW with an efficiency of 0.9. There is one fan for each floor and it is active when the outdoor air is at least 2 °C cooler than the indoor air.	Naturally driven ventilation with an opening area of 16.6 m ² representing 50 % of the window opening area. Window open when the outside air temperature is above the heating setpoint 21 °C and below the cooling setpoint 24.9 °C.	1) Mechanical cooling with indirect evaporative cooler . The fan supplies a flow rate of 611.1 l/s per room. It operates when the outdoor dry bulb temperature exceeds 22 °C and the maximum zonal temperature exceeds 24.5 °C. 2) Natural night natural ventilation activated from 10 pm to 6 am between April and October. The total operable area of the windows is 4 % of the floor area. They open if max zone temperature $T_z \geq 22$ °C and higher than the outdoor air temperature T_{oa} by 2 °C, and max T_z from the previous day ≥ 23 °C, $T_{oa} > 12$ °C and RH < 70 %	Natural night ventilation with an opening area of 25 %. As there were no occupants present during the night to manage the windows; they were intended to either stay open or remain closed throughout the night.

Moreover, the final steady state comfort state of occupants is much worse after larger temperature step changes [63,64].

In this work, the absorptivity rate Δ_{abs} (°C/h) was considered as a KPI during the absorption of the HW. Δ_{abs} is defined as the rate of change of temperature from when the SET crosses the $SET_{alert} = 28.12$ °C threshold (at time t_1) and reaches its maximum value SET_{max} at t_{max} as seen in Eq. (3).

$$\Delta_{abs} = \frac{\Delta SET}{\Delta t_{abs}} = \frac{SET_{max} - SET_{alert}}{t_{max} - t_1} \quad (3)$$

A 24 h period prior to t_1 is analyzed to check whether SET was below $SET_{alert} = 28.12$ °C. The counter on Δ_{abs} starts at t_1 only if the $SET < SET_{alert}$ during the 24 h buffer. Otherwise, additional time periods are added before t_1 and considered in the calculation of Δ_{abs} until this condition is satisfied. This is since occupants can recover from the HW during 24 h. Larger Δ_{abs} signify steeper temperature transients and worse resilience performance. During the absorption of the HW, it is additionally important to look at the final thermal state of the ambient environment expressed by SET_{max} . Thus, Δ_{abs} and SET_{max} will be analyzed together.

a) **Recovery rate:** The recovery rate Δ_{rec} (°C/h) is defined in Eq. (4) as the rate of change of temperature from when the SET declines from its maximum value SET_{max} to reach the $SET_{alert} = 28.12$ °C threshold (at time t_2):

$$\Delta_{rec} = \frac{\Delta SET}{\Delta t_{rec}} = \frac{SET_{max} - SET_{alert}}{t_2 - t_{max}} \quad (4)$$

In this work, the recovery time Δt_{rec} is defined as the time it takes by the building to go back to below the $SET_{alert} = 28.12$ °C at time t_2 from SET_{max} . Similarly to the absorptivity rate, the counter on Δ_{rec} is only stopped if the SET goes below SET_{alert} for at least 24 h. Otherwise, Δ_{rec} is calculated cumulatively until this condition is satisfied (Fig. 2). Larger recovery rates Δ_{rec} signify faster temperature transients towards the threshold conditions and better recovery performance and thus better resilience performance.

Table 4
HW characteristics per climate zone.

Climate	Period	Average HW T_{db} (°C)	Average TMY T_{db} (°C)	$T_{db, max}$ (°C)	time (h) to reach $T_{db, max}$ (°C)	Duration (days)	Global intensity (°C.days)	doS
2A	Historical (2015)	28.6	21.6	36.2	180	9 (Jan 5 – Jan 13)	20.7	0.122
	Mid-term (2059)	29.3	23.3	36.9	134	14 (Feb 9 – Feb 22)	42.2	0.150
	Long-term (2083)	30.7	18.7	43.4	227	16 (Nov 3 – Nov 18)	70.6	0.405
3A	Historical (2015)	27.9	25.4	34	132	15 (July 17 – July 31)	22.9	0.016
	Mid-term (2059)	28.5	24.9	37	445	42 (July 12 – Aug 22)	33.4	0.064
	Long-term (2084)	30.8	23.4	41	1431	95* (June 6 – Sept 18)	40.1	0.316
3B	Historical (2019)	24.1	19.2	32.7	11	5 (Aug 3 – Aug 7)	6.0	0.025
	Mid-term (2051)	24.8	19.8	39.4	444	21 (Aug 21 – Sept 10)	35.5	0.104
	Long-term (2086)	24.2	19.4	37.8	801	51* (Aug 6 – Sept 25)	65.3	0.247
4A	Historical (2002)	24.8	18.6	40.9	256	27 (July 5 – July 31)	26.3	0.201
	Mid-term (2051)	27.4	17.4	42.6	179	16 (June 27 - July 12)	25.5	0.179
	Long-term (2090)	25.0	18.3	41.7	399	45* (July 2 - Aug 15)	46.1	0.362
6A	Historical (2020)	26.7	20.8	40.9	136	7 (June 17 – June 23)	5.2	0.055
	Mid-term (2044)	24.9	22.6	42.6	325	15 (July 10 – July 24)	12.3	0.042
	Long-term (2090)	27.6	22.4	41.7	347	36* (July 7 – Aug 11)	34.5	0.232

* Longest HW duration used to calculate the doS according to Eq. (1). In climates 3A, 3B, 4A and 6A, the HW with the longest duration corresponded to the long-term HW. The exception was climate 2A where $t_{HW, longest} = 24$ days.

3. Results

3.1. Resilience performance of individual strategies in different climate zones

Figs. 3, 4, 5 and 6 illustrate the resilience performance aspects of the baseline scenario and selected passive cooling strategies for climates 2A, 3A, 3B, 4A and 6A during a) historical, b) mid-term future and c) long-term future HWs (see Table 4). The results were showcased for the most overheated zone. Table 5 illustrates the results of the different resilience

performance aspects of the strategies ranked by descending order of performance and the % of improvement. It can be generally observed that all performance aspects deteriorated with increasing doS for all climate zones and all strategies.

3.1.1. Climate 2A: hot-humid

HW impact (Fig. 3): In the baseline apartment, the most overheated zone (living room) did not exceed the acceptable SET DH threshold of $230 \pm 42^\circ\text{C}\cdot\text{h}$ during historical HWs. This was due to the combination of heavy thermal mass, which slowed internal heat storage, small window

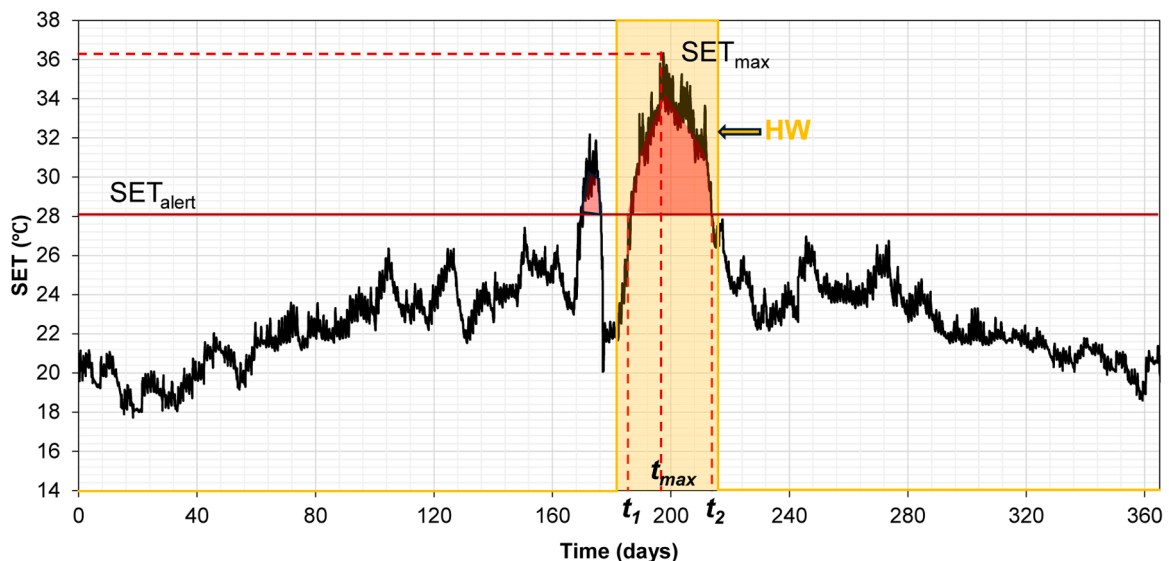


Fig. 2. Illustration of the temporal variation of SET during a HW event (yellow shaded area).

size limiting solar gains, and the short duration of the HW (9 days). The combination of cool roof coatings and cool wall paint resulted in the lowest SET DH during historical, future mid-term, and long-term HWs. For all HW periods, SET DH remained below the acceptable threshold for historical and future mid-term HWs, slightly exceeding it by 7 % during future long-term HWs. Therefore, in climate 2A, cool materials effectively minimize HW impacts on wellbeing. Additionally, cool materials kept indoor SET_{max} below the emergency threshold (32.12°C) for historical and future mid-term HWs, with a 9.5 % increase for future long-term HWs (Fig. 4). Overhangs, which cover the building perimeter, outperformed ventilative cooling (natural cross-ventilation during

occupied hours), followed by Venetian blinds and advanced glazing across all HW periods (Table 5). Notably, overhangs were more effective than Venetian blinds, as they protect not only the windows but also a significant portion of the uninsulated exterior walls.

Absorptivity rate Δ_{abs} (Fig. 5): Cool materials caused the largest reduction in Δ_{abs} among all strategies for all three HWs dampening their impact. E.g., during historical HWs, cool wall paints and cool roof coatings had Δ_{abs} of 0.006 °C/h as opposed to the baseline value of 0.040 °C/h. This is mainly due to the significant reduction in indoor temperatures compared to the baseline (cool materials had always the lowest SET_{max}, see Fig. 4) rather than absorptivity time Δt_{abs} as the latter was

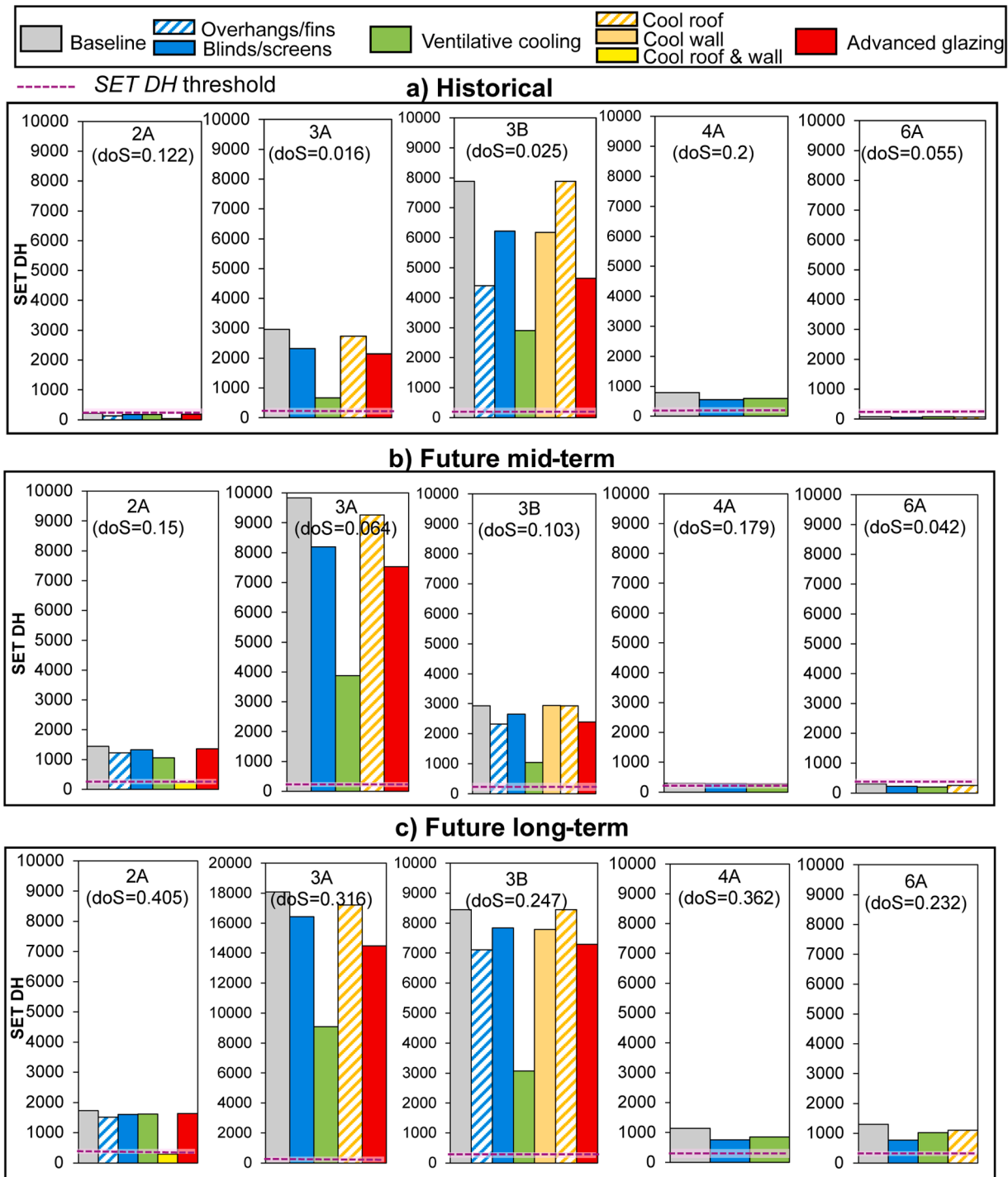


Fig. 3. Illustration of the SET DH of different cooling strategies for the different climate zones (note that the y-axis scales in c) 3A is different to improve the visibility of the results).

the shortest for cool materials as opposed to the other strategies for all three HW periods (e.g., cool materials: $\Delta SET = SET_{max} - SET_{thresh} = 4\text{ }^\circ\text{C}$ during 241 h vs baseline: $7.2\text{ }^\circ\text{C}$ during 294 h during future mid-term HW).

As for solar shading, both strategies reduced Δ_{abs} compared to the baseline during historical and future mid-term HWs due to lower ΔSET and more significantly longer Δt_{abs} (e.g., overhangs: $1.7\text{ }^\circ\text{C}$ during 187 h vs baseline: $2.6\text{ }^\circ\text{C}$ during 65 h for historical HWs). Both strategies had lower SET_{max} than the baseline for all three HW periods (3 % and 1 % reduction for overhangs and blinds respectively) but remained above $SET_{emergency}$. No improvement was noted for future long-term HWs given

lower ΔSET with shorter Δt_{abs} compared to the baseline (e.g., blinds: $9.7\text{ }^\circ\text{C}$ during 314 h vs baseline: $10.1\text{ }^\circ\text{C}$ during 316 h). Both overhangs and venetian blinds performed similarly except during historical HWs where overhangs had much lower Δ_{abs} than venetian blinds ($0.009\text{ }^\circ\text{C/h}$ vs. $0.033\text{ }^\circ\text{C/h}$) due to 65 % higher Δt_{abs} .

Ventilative cooling had the highest absorptivity rate among all strategies for the three HW periods even exceeding the baseline in the case of future mid-term HWs ($0.026\text{ }^\circ\text{C/h}$ vs. the baseline value of $0.023\text{ }^\circ\text{C/h}$). This is due to shorter absorptivity times Δt_{abs} (the second shortest Δt_{abs} after cool materials) in combination with larger ΔSET which was comparable to the baseline (e.g., $2.5\text{ }^\circ\text{C}$ during 65 h vs baseline: 2.6

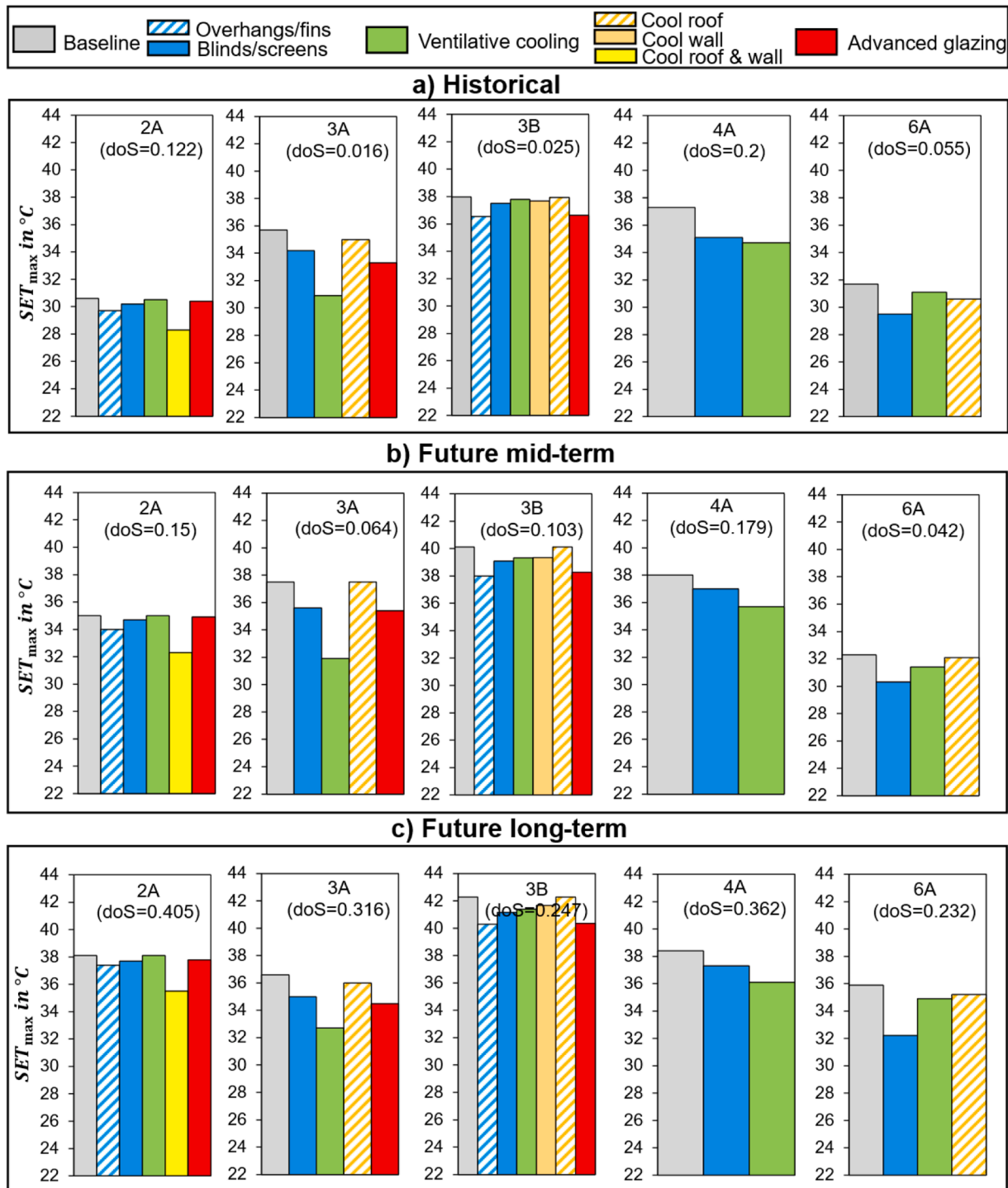


Fig. 4. Illustration of SET_{max} of different cooling strategies for the different climate zones.

°C during 65 h during historical HW). This can be seen by looking at Fig. 4. Ventilative cooling could not reduce SET_{max} compared to the baseline for all three HWs. Ventilative cooling was closely followed by advanced glazing strategies for the same reasons. However, advanced glazing technologies had slightly lower ΔSET reducing their Δ_{abs} by an average of 5.6 %.

Recovery rate Δ_{rec} (Fig. 6): During historical HWs, venetian blinds, ventilative cooling and advanced glazing slightly reduced Δ_{rec} given that their recovery time Δt_{rec} was equal to that of the baseline with lower ΔSET (Fig. 4). Overall, they did not significantly impact the recovery of the building. The use of overhangs significantly improved the Δ_{rec}

compared to the baseline increasing it by 43.4 % given a substantial decrease in Δt_{rec} (118 h with overhangs vs. 319 h for the baseline) in tandem with a reduction in ΔSET . Thus, the use of overhangs, can help recover the building quickly and restore it to safer conditions. However, cool wall paints and cool roof coatings reduced Δ_{rec} by 80 %. This is since the reduction in ΔSET was higher than the reduction in Δt_{rec} (overhangs: 0.3 °C in 190 h vs baseline: 2.6 °C in 319 h). However, this effect is negligible since the SET decrease was only by 0.3°C over a duration of 8 days.

During future mid-term HWs, the use of overhangs, venetian blinds and advanced glazing did not significantly impact the recovery capacity

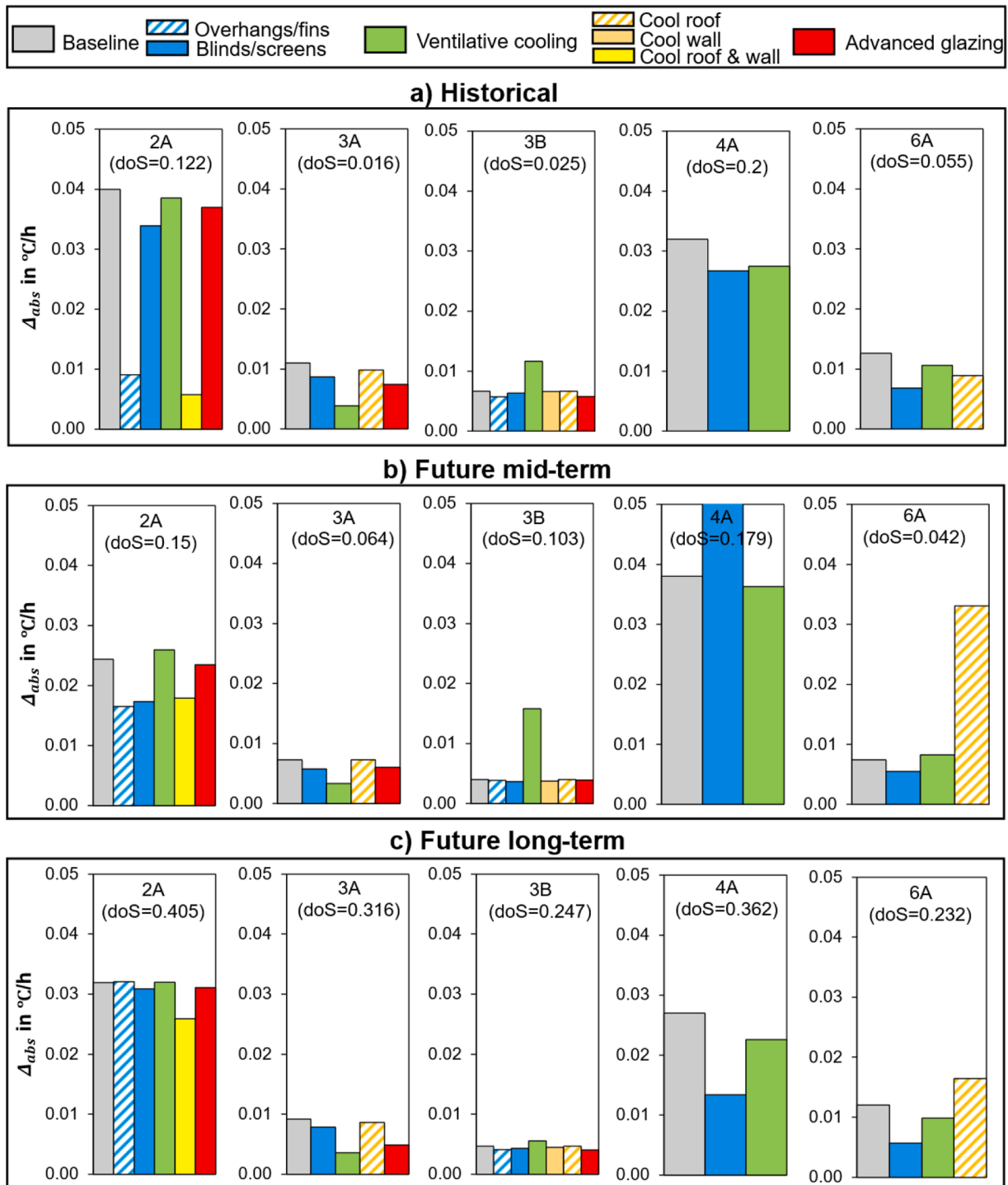


Fig. 5. Illustration of the Δ_{abs} of different cooling strategies for the different climate zones.

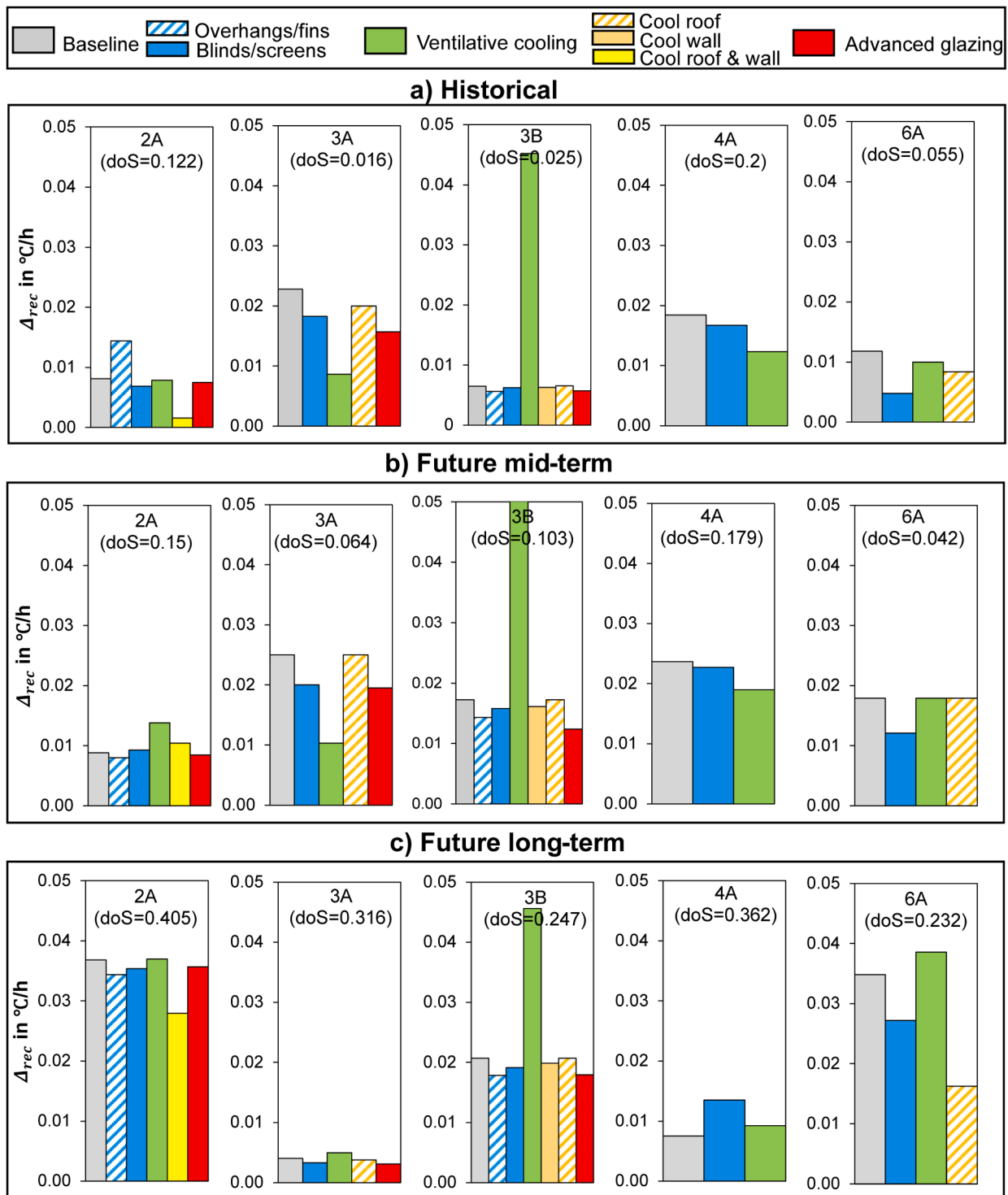


Fig. 6. Illustration of the Δ_{rec} of different cooling strategies for the different climate zones.

of the building. The use of cool materials and ventilative cooling increased Δ_{rec} by 12 % and 36 %. This is due to a 49.4 % and 37.7 % reduction in Δt_{rec} and a 40.3 % and 2 % decrease in ΔSET compared to the baseline respectively.

During future long-term HWs, the use of overhangs, venetian blinds, ventilative cooling and advanced glazing did not significantly impact the recovery. However, the use of cool materials reduced Δ_{rec} by 24 % compared to the baseline. This is since cool materials only reduced ΔSET compared to the baseline (7.5 °C vs. 10.1 °C) with no change in Δt_{rec} .

3.1.2. Climate 3A: warm-humid

HW impact (Fig. 3): It was observed that the SET DH for all three HWs significantly exceeded the permissible threshold of $230 \pm 42^\circ\text{C}\cdot\text{h}$, even with the implementation of passive cooling strategies. This was due to the shorter heat events in climate 3A, where heat gradually accumulated in the space before the HWs began. With the building's high thermal mass, heat dissipation was also delayed. Furthermore, climate 3A experienced relatively longer HWs compared to other climates (Table 4). Among all strategies, ventilative cooling (mechanical-driven ventilation using an axial fan, activated when the outdoor air

Table 5
Ranking of resilient cooling strategies per climate zone with % of improvement with respect to the baseline (n/i = no improvement).

Resilience aspects	Climate zones				
	2A	3A	3B	4A	6A
a) Historical HWs					
HW impact (<i>SET DH</i>)	Cool roof+wall (85 %) Overhangs (40 %) Ventilative cooling (18 %) Venetian blinds (17 %) Advanced glazing (15 %)	Ventilative cooling (77 %) Advanced glazing (28 %) Solar shading (22 %) Cool roof (8 %)	Ventilative cooling (63 %) Overhangs & fins (44 %) Advanced glazing (41 %) Cool walls (22 %) Exterior screens (21 %) Cool roof (n/i)	Solar shading (30 %) Ventilative cooling (26 %)	Solar shading (30 %) Cool roof (14 %) Ventilative cooling (8 %)
Absorption rate (Δ_{abs})	Cool roof+wall (86 %) Overhangs (77 %) Venetian blinds (18 %) Advanced glazing (8 %) Ventilative cooling (4 %)	Ventilative cooling (54 %) Advanced glazing (32 %) Solar shading (21 %) Cool roof (11 %)	Overhangs & fins (14 %) Advanced glazing (13 %) Exterior screens (n/i) Cool walls (n/i) Cool roof (n/i) Ventilative cooling (n/i)	Solar shading (17 %) Ventilative cooling (12 %)	Solar shading (28 %) Cool roof (25 %) Ventilative cooling (n/i)
Recovery rate (Δ_{rec})	Overhangs (44 %) Ventilative cooling (n/i) Advanced glazing (n/i) Venetian blinds (n/i) Cool roof+wall (n/i)	All strategies: n/i	Ventilative cooling (85 %) Cool roof (n/i) Cool walls (n/i) Overhangs & fins (n/i) Exterior screens (n/i) Advanced glazing (n/i)	All strategies: n/i	All strategies: n/i
b) Future mid-term HWs					
HW impact (<i>SET DH</i>)	Cool roof+wall (83 %) Ventilative cooling (26 %) Overhangs (16 %) Venetian blinds (8 %) Advanced glazing (6 %)	Ventilative cooling (61 %) Advanced glazing (23 %) Solar shading (17 %) Cool roof (6 %)	Ventilative cooling (65 %) Overhangs & fins (21 %) Advanced glazing (18 %) Exterior screens (10 %) Cool walls (n/i) Cool roof (n/i) All strategies: n/i	Ventilative cooling (8 %) Solar shading (5 %)	Solar shading (28 %) Ventilative cooling (33 %) Cool roof (18 %)
Absorption rate (Δ_{abs})	Cool roof+wall (27 %) Overhangs (32 %) Venetian blinds (29 %) Advanced glazing (4 %) Ventilative cooling (n/i)	Ventilative cooling (61 %) Advanced glazing (20 %) Solar shading (17 %) Cool roof (4 %)	All strategies: n/i	Ventilative cooling (5 %) Solar shading (n/i)	Solar shading (26 %) Ventilative cooling (n/i) Cool roof (n/i)
Recovery rate (Δ_{rec})	Ventilative cooling (57 %) Cool roof+wall (16 %) Venetian blinds (5 %) Overhangs: n/i Advanced glazing: n/i	All strategies: n/i	Ventilative cooling (85 %) Cool roof (n/i) Cool walls (n/i) Overhangs & fins (n/i) Exterior screens (n/i) Advanced glazing (n/i)	All strategies: n/i	All strategies: n/i
c) Future long-term HWs					
HW impact (<i>SET DH</i>)	Cool roof+wall (83 %) Overhangs (12 %) Venetian blinds (7 %) Ventilative cooling (6 %) Advanced glazing (5 %)	Ventilative cooling (50 %) Advanced glazing (20 %) Solar shading (9 %) Cool roof (5 %)	Ventilative cooling (64 %) Overhangs & fins (16 %) Advanced glazing (14 %) Exterior screens (8 %) Cool walls (8 %) Cool roof (n/i) All strategies: n/i	Solar shading (35 %) Ventilative cooling (26 %)	Solar shading (40 %) Ventilative cooling (22 %) Cool roof (15 %)
Absorption rate (Δ_{abs})	Cool roof+wall (19 %) Venetian blinds (6 %) Overhangs: n/i Ventilative cooling: n/i Advanced glazing: n/i	Ventilative cooling (61 %) Advanced glazing (47 %) Solar shading (15 %) Cool roof (6 %)	All strategies: n/i	Solar shading (50 %) Ventilative cooling (16 %)	Solar shading (58 %) Ventilative cooling (18 %) Cool roof (n/i)
Recovery rate (Δ_{rec})	All strategies: n/i	Ventilative cooling (25 %) Other strategies: n/i	Ventilative cooling (55 %) Cool roof (n/i) Cool walls (n/i) Overhangs & fins (n/i) Exterior screens (n/i) Advanced glazing (n/i)	Solar shading (44 %) Ventilative cooling (19 %)	Ventilative cooling (8 %) Solar shading (n/i) Cool roof (n/i)

temperature is 2°C lower than the internal temperature, Table 3) achieved the lowest SET DH for all three HWs. Ventilative cooling reduced SETmax by 4.8°C, 5.6°C, and 3.9°C compared to the baseline for historical, future mid-term, and long-term HWs, respectively. It was followed by advanced glazing (ultra-selective double-glazed windows with SHGC = 0.3, VT = 0.64, U = 1.2 W/m²·K), solar shading (external roller blinds with ST of 13 % and SR of 0.41, activated when solar irradiance exceeds 300 W/m²), and finally cool roof coatings (SR of 0.5, infrared emittance of 0.86). The percentage improvements for the different strategies can be seen in Table 5.

The trends of reduction of SETmax followed the same trends as the SET DH. Advanced glazing reduced SETmax by 2.4 °C, 2.1 °C, 2.1 °C compared to the baseline for historical, future mid-term and long-term respectively. Solar shading reduced SETmax by 1.5 °C, 1.9 °C, and 1.6

°C compared to the baseline for historical, future mid-term and long-term respectively. Cool materials on the roof reduced SETmax by 0.7 °C, 0.1 °C, 0.6 °C compared to the baseline for historical, future mid-term and long-term respectively. However, SETmax remained above SETemergency for all strategies during all HWs except for ventilative cooling where SETemergency threshold was only exceeded during future long-term HWs.

Absorptivity rate Δ_{abs} (Fig. 5): The trends of Δ_{abs} followed the same trends as the SET DH and SETmax. Ventilative cooling reduced (and thus improved) Δ_{abs} followed by advanced glazing, solar shading and cool materials. These strategies reduced the absorptive capacity by mainly reducing ΔSET and some by increasing Δt_{abs} . For example, ventilative cooling and advanced glazing increased Δt_{abs} by 381 h and 396 h during future long-term HW respectively. The other strategies did not

significantly impact Δt_{abs} .

Recovery rate Δ_{rec} (Fig. 6): The trends of Δ_{rec} followed the same trends as the SET_{DH} and SET_{max} and Δ_{abs} for historical and future mid-term HWs. Ventilative cooling reduced (and thus degraded) Δ_{rec} followed by advanced glazing, solar shading and cool materials. This occurred due to the strategies reducing ΔSET without impacting Δt_{rec} . This led to a slower more gradual recovery. For future long-term HWs, the trends of Δ_{rec} differed. Advanced glazing, solar shading and cool materials reduced Δ_{rec} by 25 %, 17.5 % and 5.5 % but ventilative cooling increased Δ_{rec} by 25 % due to a significant decrease in Δt_{rec} by 1163 h.

3.1.3. Climate 3B: warm-dry

HW impact (Fig. 3): The SET_{DH} in this building for all 3 HW periods exceeded the permissible SET_{DH} threshold of 230 ± 42 °C.h significantly even with the implementation of strategies. This can be due to the design of the single-family home representing the 2019 vintage with high insulation and less air infiltration, which would be often overheated throughout the year. The latter had U-values of 2.7, 3.7 and 5.5 W/m².K for the walls, floor and roof respectively in addition to light thermal mass. Ventilative cooling (Natural driven ventilation operational when the outside air temperature is above the heating setpoint 21 °C and below the cooling setpoint 24.9 °C) reduced SET_{DH} the most, followed by solar shading (Horizontal overhang on south façade, Vertical fin on southern side of the window on the east and west façades with depth of 0.5), advanced glazing (Electrochromic dynamic glazing, SHGC and VT switched from light (0.5, 0.75) to dark (0.1, 0.15) when $GSI > 100$ W/m² on window, $U = 1.7$ W/m².K) for the 3 HWs. Exterior screen and cool walls paint and cool roof coating (solar reflectance of 0.6, infrared emittance of 0.9) performed similarly for the 3 HWs. Cool roof did not bring any improvement to the SET_{DH} in any of the HW periods. Cool walls did not bring any improvement to the SET_{DH} only in the future mid-term HW. The improvement % can be seen in Table 5. Overhangs outperformed exterior screens as was the case with climate 2A.

The strategies reducing SET_{max} the most were overhangs+fans and advanced glazing technologies by 1.5 °C and 1.4 °C for historical HW, 2.1 °C and 1.8 °C for future mid-term HW, 2 °C and 1.9 °C for future long-term HW respectively. This was followed by exterior screens, ventilative cooling and cool walls which reduced SET_{max} similarly by 0.5 °C, 0.2 °C, 0.3 °C for historical HW, 1 °C, 0.8 °C, 0.7 °C for future mid-term HW, 1.1 °C, 0.9 °C, 0.6 °C for future long-term HW respectively. Cool roof did not reduce SET_{max} .

Absorptivity rate Δ_{abs} (Fig. 5): It can be observed that in climate 3B, the absorptivity rates of all the strategies except for ventilative cooling did not significantly change Δ_{abs} from the baseline value for all three HW periods. Δt_{abs} was not impacted and the slight decrease in ΔSET did not cause changes in the Δ_{abs} . Ventilative cooling increased Δ_{abs} by 40 %, 73 % and 17 % for historical, future mid-term and future long-term HWs respectively compared to the base case. While ventilative cooling reduced ΔSET by 0.2 °C, 0.8 °C and 0.9 °C, it decreased Δt_{abs} more significantly.

Recovery rate Δ_{rec} (Fig. 6): For historical and future mid-term HWs, all the strategies (except for ventilative cooling) did not influence the Δ_{rec} compared to the baseline. Ventilative cooling sped up Δ_{rec} significantly by 85 % and due to a decrease in Δt_{rec} by 1302 h. For future long-term HWs, overhangs+fans and advanced glazing slowed down Δ_{rec} by 14 % and exterior blinds by 8 %. Ventilative cooling sped up Δ_{rec} significantly by 55 % and due to a decrease in Δt_{rec} by 397 h. The rest of the strategies did not impact Δ_{rec} .

3.1.4. Climate 4A: mixed-humid

HW impact (Fig. 3): The SET_{DH} for all 3 HW periods exceeded the permissible SET_{DH} threshold of 230 ± 42 °C.h even with the implementation of strategies. This can be due to heat events occurring prior to the HW itself causing some heat storage that the heavy thermal mass of the building could not fully dissipate. The implementation of solar shading (exterior automated screen that close for 15 min with the solar

radiation > 250 W/m²) and ventilative cooling (indirect evaporative cooler + night ventilation) decreased SET_{DH} compared to the baseline with ventilative cooling outperforming solar shading (Table 5). The trends of SET_{max} were proportional with ventilative cooling causing a larger reduction compared to the baseline (Fig. 4). E.g., in future long term HWs, ventilative cooling reduced SET_{max} by 2.3 °C while solar shading reduced it by 0.8 °C.

Absorptivity rate Δ_{abs} (Fig. 5): For historical and future long-term HWs, ventilative cooling and solar shading slowed down Δ_{abs} due to a reduction of ΔSET which was larger than the reduction in Δt_{abs} . Solar shading had a lower Δ_{abs} since it did not significantly reduce Δt_{abs} as was the case with ventilative cooling. During future mid-term HWs, solar shading increased Δ_{abs} due to 86 h reduction in Δt_{abs} . This increase was larger than the rate of reduction in ΔSET of 10 %.

Recovery rate Δ_{rec} (Fig. 6): For historical and future mid-term HWs, ventilative cooling and solar shading reduced Δ_{rec} due to a reduction of ΔSET for a similar Δt_{rec} as the baseline case. Ventilative cooling had a lower Δ_{rec} since it did not significantly reduce Δt_{rec} as was the case with solar shading. During future long-term HWs, solar shading increased Δ_{rec} due to 686 h reduction in Δt_{rec} . This increase was larger than the rate of reduction in ΔSET of 11 %.

Particularly for climate 3B and 4A, with increasing doS , the resilience KPIs improved for all strategies going from historical to future mid-term HWs. While this seems counterintuitive, it is due to larger sky coverage and a reduction in solar radiation during the future mid-term HW as predicted by the weather generation method. For future long-term, values deteriorated once more.

3.1.5. Climate 6A: cold-humid

HW impact (Fig. 3): The SET_{DH} was lower than the permissible SET_{DH} threshold of 230 ± 42 °C.h for historical HW (even with the base case) and future mid-term HW with the implementation of strategies. The performance of the three strategies were similar during historical and future mid-term HWs. During future long-term HWs, solar shading performed best followed by ventilative cooling and cool materials (Table 5). The trends of SET_{max} were proportional with solar shading causing the largest reduction compared to the baseline (Fig. 4). For e.g., in future long term HWs, solar shading reduced SET_{max} by 4 °C while ventilative cooling and cool roof coatings reduced it by 1 °C and 0.8 °C respectively.

Absorptivity rate Δ_{abs} (Fig. 5): For historical HWs, all strategies decreased Δ_{abs} compared to the base case due to a reduction of ΔSET . Solar shading had a lower Δ_{abs} since it had the lowest ΔSET of 1.5 °C followed by ΔSET of 3.1 °C and 2.6 °C for ventilative cooling and cool materials respectively. During future mid-term and long-term HWs, solar shading and ventilative cooling decreased Δ_{abs} with solar shading outperforming ventilative cooling. This is due to the reduction in ΔSET which was larger than the decrease in Δt_{abs} . Cool materials caused an increase in Δ_{abs} compared to the baseline due a large decrease in Δt_{abs} (e.g., 216 h during future long-term HWs) accompanied by ΔSET that was slightly smaller than that of the baseline.

Recovery rate Δ_{rec} (Fig. 6): For historical HWs, all strategies reduced Δ_{rec} due to a reduction of ΔSET for a similar Δt_{rec} as the baseline case. For future mid-term HWs, solar shading reduced Δ_{rec} due to a reduction in ΔSET for a slightly shorter Δt_{rec} (i.e., 50 h). Ventilative cooling caused no change (reduction in ΔSET had the same rate as the decrease in Δt_{rec}). Cool roof coatings reduced Δ_{rec} the most due to ΔSET similar to the baseline for a longer Δt_{rec} (i.e., 240 h). For future long-term HWs, solar shading reduced Δ_{rec} due to a reduction of ΔSET that was higher than the reduction in Δt_{rec} compared the baseline. Cool materials reduced Δ_{rec} due to increased Δt_{rec} compared the baseline with no improvement in ΔSET . Ventilative cooling improved Δ_{rec} by shortening both Δt_{rec} and reducing ΔSET .

4. Discussion

4.1. Resilience performance of individual strategies

Fig. 7 showcases the three resilience performance indicators normalized with respect to their baseline values ($SET\ DH^*$, Δ_{abs}^* , Δ_{rec}^*) for the cooling strategies per climate zone. Smaller $SET\ DH^*$ (<1) signify a lower HW impact, smaller Δ_{abs}^* (<1) signifies a slower absorptivity (more gradual) and a larger Δ_{rec}^* (>1) signifies a faster recovery. The graphical representation in Fig. 7 allows to analyze the full resilience spectrum of each strategy and draw conclusions regarding its suitability for a climate.

Solar Shading: Solar shading strategies, such as overhangs, fins, and blinds, reduce solar heat gains by casting shadows or blocking solar radiation on glazing. During historical HWs, solar shading successfully reduced both HW impact and absorptivity rates across all climate zones. Overhangs and fins outperformed automated blinds in climates 2A and 3B, as they provided a constant shadow, reducing solar gains more effectively. In future HWs, all solar shading strategies continued to reduce HW impact and absorptivity but with less effectiveness due to longer durations, higher temperatures, and increased solar radiation. However, solar shading strategies did not improve recovery times, as they only address heat gains without altering the heat transfer mechanisms (e.g., convection or conduction) that control the rate of heat dissipation.

Ventilative cooling: Ventilative cooling reduces indoor temperatures by bringing in cooler outdoor air through natural or mechanical ventilation when conditions are favorable. During historical HWs, it effectively lowered HW impact, absorptivity rates, and, in some cases, recovery times across all climate zones, with the greatest success in 3B, followed by 3A. The performance variation is due to outdoor temperature conditions and building design. In climate 3B, ventilative cooling was available 24/7 when outdoor temperatures were below 25°C, which often occurred during the day, making it highly efficient and aiding fast recovery. In climate 3A, despite less favorable conditions, it still worked well due to acceptable diurnal temperature gradients and heavy thermal mass, leading to slower absorptivity. In climates 2A, 4A, and 6A, the impact was less significant as the buildings weren't as overheated. In future HWs, ventilative cooling continues to perform well across all climates, with only a slight reduction in effectiveness due to increased HW intensity and duration, and fewer favorable conditions for its activation.

Cool materials: Cool materials lower façade temperatures by reflecting solar radiation, reducing indoor peak temperatures. During historical HWs, they effectively reduced HW impact and absorptivity across climates 2A, 3A, 3B, and 6A, with the best results in 2A. This was due to high solar reflectance (0.8), infrared emittance (0.9), extensive coverage, high thermal mass, and low WWR (17%). In 3A and 6A, their effectiveness was reduced as they covered only the roof, had lower solar reflectance (0.5), and the building was well insulated. In 3B, cool roofs were less efficient than cool walls due to light insulation, low thermal mass, and a lower solar reflectance coating (0.6). In future mid- and long-term HWs, cool materials remain effective, especially in 2A. In 2A, HW impact reduction stays consistent, but absorptivity rate reductions drop significantly due to smaller temperature gradient changes and increased HW duration. In 3A, performance is similar to historical HWs with a slight decline due to a less severe increase in HW duration. In 6A, cool materials continue to reduce HW impact but no longer improve absorptivity due to the increased duration of HWs. In 3B, their impact is minimal, as future HWs last 21–51 days with temperatures exceeding 39°C, making cool materials ineffective due to the apartment's light thermal mass and insulation.

When it comes to recovery, cool materials did not speed up the recovery rate from any HW period in any climate as they did not influence the recovery time. They could not dissipate the heat faster from the

building. This is since coating only address heat gains but does not modify the underlying mechanisms of heat transfer (e.g., convection or conduction) that control the rate of heat dissipation.

Advanced glazing: Advanced glazing technologies use special coatings to reduce solar heat gains and indoor maximum temperatures. During historical HWs, they reduced HW impact and absorptivity rates in climates 2A, 3A, and 3B, though least effectively in 2A. This was likely due to the small glazing area (7 m² vs. 43 m² floor area) and a limited U-value reduction (36%). In 3A, advanced glazing performed better despite a low WWR, thanks to ultra-selective double glazing with low-emissivity coatings, which allowed visible light while blocking heat gains. In 3B, it was most effective at reducing HW impact and second best for absorptivity rates. This was due to dynamic glazing that adjusted based on solar radiation, switching between dark (SHGC 0.1, VT 0.15) and light (SHGC 0.5, VT 0.75) when solar radiation exceeded 100 W/m², effectively blocking unwanted heat.

During future mid- and long-term HWs, advanced glazing continues to reduce HW impact and absorptivity rates relative to the baseline but with lower effectiveness due to prolonged exposure to solar gains from increased HW doS. Its performance remains weakest in 2A and declines further in 3B compared to 3A. This is due to the light thermal mass and insulation in 3B, where advanced glazing, like cool materials, becomes less effective. For recovery, advanced glazing, similar to cool materials, offers no benefits in any HW period, as it only reduces temperature spikes without affecting recovery times.

5. Limitations

This study simulated different cooling strategies and quantitatively assessed their full resilience spectrum using different KPIs that simultaneously describe different resilience aspects. This allowed to rank the different strategies per climate and HW period (Table 5). However, this study does not allow to draw cross-climate comparisons. This is since different buildings and design of cooling strategies were simulated, which can impact resilience performance as seen in [65]. Moreover, in some climates (3B, 4A), it was seen the future mid-term HW was less severe than the historical HWs (lower HW impact, Fig. 3). This is due to limitations regarding the methodology of generating the climate files detailed in [31]. This study was an aggregation of the simulation activities conducted in the framework of IEA EBC Annex 80. Thus, simulations were conducted on a selection of climates on the moderate end of the spectrum. Moreover, not all the cooling strategies were simulated in all the climates. Consequently, more insight is needed on the resilience performance of all cooling strategies in all climates including more extreme climates (0A, 0B, 7).

Another limitation is the exclusive focus on the highest emission scenario RCP 8.5. This approach was chosen to evaluate the proposed measures under the most challenging conditions. However, this does not account for the potential variability in outcomes under more optimistic scenarios, such as those associated with lower emission pathways. Including a broader range of emission scenarios, particularly lowest emission scenario, would provide a clearer understanding of the improvements in resilience achieved by different measures across varying climate conditions. Future work will aim to address this limitation by incorporating both worst-case and best-case scenarios to offer a more comprehensive evaluation of the proposed measures. Moreover, while the use of an averaged SET_{alert} threshold to calculate HW impact provides a unified benchmark for resilience assessment across diverse climates, it may not fully capture localized variations in thermal adaptation and comfort preferences. Future studies could explore the use of climate-specific thresholds to better account for the unique thermal responses of populations in specific environmental contexts. Finally, this study does not account for urban heat island (UHI) effects. Most weather files used in the analysis are sourced from airport open-space measurement sites, which may not accurately capture the actual or peak UHI conditions experienced in densely built urban areas. This

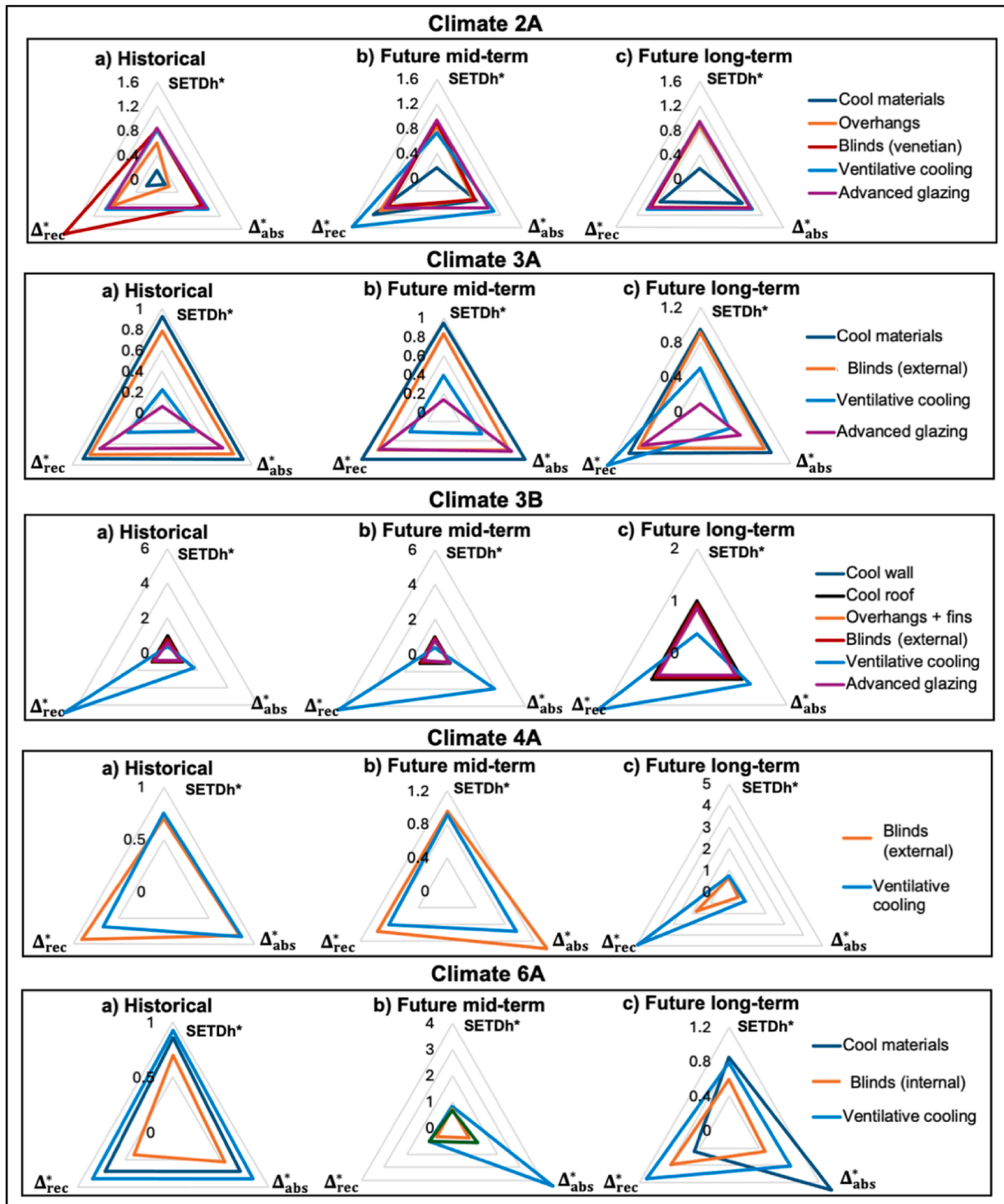


Fig. 7. Radar chart of the resilience performance spectrum (i.e., normalized KPIs: SET DH*, Δ_{abs}^* and Δ_{rec}^*) of the different cooling strategies for the different climate zones and HW periods.

discrepancy could lead to an underestimation of localized heat stress and its impacts on resilience strategies. Future work should consider incorporating site-specific UHI data or high-resolution urban climate models to address this gap.

6. Conclusions

In this work, the resilience performance of individual passive cooling strategies was assessed for climates 2A, 3A, 3B, 4A and 6A and 3

different HW periods (historical, future mid-term and future long-term). This work is an aggregation and analysis of the simulations conducted by IEA EBC's Annex 80: Resilient Cooling of Buildings. The main conclusions are summarized below:

- Deploying solar shading at the start of a HW or preemptively offers moderate benefits in all climates (improvements < 50%). As doS increases, shading enhances resilience but with reduced effectiveness (improvements < 30%). However, it does not accelerate recovery,

nor can it fully mitigate HW impacts to achieve a resilient building. Similar conclusions were drawn in [20] where external solar shading improved zone level resilience in climate 6A but could not reach building-level resilience.

- Ventilative cooling strategies help reduce HW impact and absorptivity rates across all climates, performing especially well in 3A and 3B. Unlike other strategies, they accelerate recovery times and rates. Their effectiveness depends on favorable temperature gradients and building thermal mass. While future HWs may reduce temperature gradients, their performance remains largely consistent.
- Cool materials can be an efficient strategy in reducing HW impact and its absorptivity rate in all climates and during all HW periods, especially in climate zone 2A where it reduced the *SET DH* to acceptable levels as was seen in [24]. Climate zone 3B benefited from cool materials only slightly during historical HWs and not at all during future mid-term and long-term HWs. Cool materials did not speed up recovery from HWs.
- Advanced glazing effectively reduces HW impact and absorptivity rates across all climates, especially in 3A. In 2A, its benefits were minimal during historical HWs and absent in future mid- and long-term HWs. It does not accelerate recovery. In 3A [19], advanced glazing reduced overheating but less so during longer HWs. In 2A [24], the reduction in *SET DH* was also moderate due to the use of advanced glazing (improvements < 30 %).

While solar shading, cool materials, and advanced glazing effectively reduce heatwave impacts and absorption rates, ventilative cooling stands out as the most versatile strategy that can also accelerate recovery after a heatwave, particularly in climates with favorable day-night temperature gradients. Since no single strategy could single handedly mitigate HW effects, future work includes combining multiple cooling strategies with ventilative cooling in different climates and giving insight on the most resilient combinations.

CRedit authorship contribution statement

Douaa Al-Asaad: Writing – review & editing, Writing – original draft, Visualization, Validation, Supervision, Software, Project administration, Methodology, Investigation, Formal analysis, Data curation, Conceptualization. **Abantika Sengupta:** Methodology, Formal analysis, Data curation. **Peihang An:** Methodology, Formal analysis, Data curation. **Hilde Breesch:** Writing – review & editing, Supervision, Software, Project administration, Methodology, Investigation, Conceptualization. **Afshin Afshari:** Software, Investigation, Formal analysis, Data curation. **Deepak Amaripadath:** Writing – review & editing, Software, Methodology, Investigation, Formal analysis, Data curation. **Shady Attia:** Methodology, Investigation, Formal analysis, Data curation, Conceptualization. **Fuad Baba:** Writing – review & editing, Methodology, Investigation, Formal analysis, Data curation. **Vincenzo Corrado:** Writing – review & editing, Methodology, Investigation, Formal analysis, Conceptualization. **Letícia Eli:** Methodology, Investigation, Formal analysis, Data curation. **Amanda F. Krelling:** Writing – review & editing, Methodology, Investigation, Formal analysis, Data curation. **Sang Hoon Lee:** Writing – review & editing, Methodology, Investigation, Formal analysis, Data curation. **Ronnen Levinson:** Writing – review & editing, Methodology, Investigation, Formal analysis, Data curation. **Marcelo Olinger:** Methodology, Investigation, Formal analysis, Data curation. **Mamak P. Tootkaboni:** Writing – review & editing, Methodology, Investigation, Formal analysis, Data curation. **Liangzhu (Leon) Wang:** Writing – review & editing, Methodology, Investigation, Formal analysis, Data curation. **Chen Zhang:** Project administration, Methodology, Investigation, Conceptualization. **Michele Zinzi:** Methodology, Formal analysis, Conceptualization.

Declaration of competing interest

The authors declare that they have no known competing financial interests or personal relationships that could have appeared to influence the work reported in this paper.

Acknowledgements

The authors would like to thank the operating agents and the participants of the IEA-EBC Annex 80: Resilient Cooling of Buildings. This work was supported by the Brazilian Federal Agency for the Support and Evaluation of Graduate Education (CAPES)—Financing Code 001—, and the National Council for Scientific and Technological Development (CNPq) and by the Flanders Innovation and Entrepreneurship (VLAIO) in the Flux 5.0 Project ‘ReCOVer++: Improving resilience of buildings to overheating.’ It was also supported by the Assistant Secretary for Energy Efficiency and Renewable Energy, Building Technologies Office, of the U.S. Department of Energy under Contract No. DE-AC02-05CH11231.

Data availability

Data will be made available on request.

References

- [1] C. Mora, B. Dousset, I.R. Caldwell, F.E. Powell, R.C. Geronimo, C.R. Bielecki, C.W. W. Counsell, B.S. Dietrich, E.T. Johnston, L.V. Louis, M.P. Lucas, M.M. Mckenzie, A.G. Shea, H. Tseng, T.W. Giambelluca, L.R. Leon, E. Hawkins, C. Trauernicht, Global risk of deadly heat, *Nat. Clim. Change* 7 (2017) 501–506, <https://doi.org/10.1038/nclimate3322>, 2017 7:7.
- [2] AR6 Synthesis Report: Climate Change 2023, <https://www.ipcc.ch/report/ar6/syr/>.
- [3] K.G. Arbutnot, S. Hajat, The health effects of hotter summers and heat waves in the population of the United Kingdom: a review of the evidence, *Environ. Health* 16 (2017) 1–13, <https://doi.org/10.1186/S12940-017-0322-5>, 2017 16:1.
- [4] N. Watts, M. Amann, N. Arnell, S. Ayeb-Karlsson, J. Beagley, K. Belesova, M. Boykoff, The 2020 report of the lancet countdown on health and climate change: responding to converging crises, *Lancet* 397 (2021) 129–170, [https://doi.org/10.1016/S0140-6736\(20\)32290-X](https://doi.org/10.1016/S0140-6736(20)32290-X).
- [5] K. Joshi, A. Khan, P. Anand, J. Sen, Understanding the synergy between heat waves and the built environment: a three-decade systematic review informing policies for mitigating urban heat island in cities, *Sustain. Earth Rev.* 7 (2024) 1–23, <https://doi.org/10.1186/S42055-024-00094-7>, 2024 7:1.
- [6] C. Prodhomme, S. Matera, C. Ardilouze, R.H. White, L. Batté, V. Guemas, G. Fragkoulidis, J. García-Serrano, Seasonal prediction of European summer heatwaves, *Clim. Dyn.* 58 (2022) 2149–2166, <https://doi.org/10.1007/S00382-021-05828-3>.
- [7] A. Pathan, A. Mavrogianni, A. Summerfield, T. Oreszczyn, M. Davies, Monitoring summer indoor overheating in the London housing stock, *Energy Build.* 141 (2017) 361–378, <https://doi.org/10.1016/J.ENBUILD.2017.02.049>.
- [8] I. Tsoulou, C.J. Andrews, R. He, G. Mainelis, J. Senick, Summertime thermal conditions and senior resident behaviors in public housing: A case study in Elizabeth, NJ, USA, *Build Environ.* 168 (2020), <https://doi.org/10.1016/j.buildenv.2019.106411>.
- [9] A. Baniassadi, D.J. Sailor, C.R. Olenick, Indoor air quality and thermal comfort for elderly residents in Houston TX—A case study, in: 2018. <https://doi.org/10.14305/ibpc.2018.ie-2.04>.
- [10] M. Vellei, A.P. Ramallo-González, D. Coley, J. Lee, E. Gabe-Thomas, T. Lovett, S. Natarajan, Overheating in vulnerable and non-vulnerable households, *Build. Res. Inform.* 45 (2017), <https://doi.org/10.1080/09613218.2016.1222190>.
- [11] M. Zuurbier, J.A.F. van Loenhout, A. le Grand, F. Greven, F. Duijm, G. Hoek, Street temperature and building characteristics as determinants of indoor heat exposure, *Sci. Total Environ.* 766 (2021), <https://doi.org/10.1016/j.scitotenv.2020.144376>.
- [12] R. Gupta, A. Howard, M. Davies, A. Mavrogianni, I. Tsoulou, N. Jain, E. Oikonomou, P. Wilkinson, Monitoring and modelling the risk of summertime overheating and passive solutions to avoid active cooling in London care homes, *Energy Build.* 252 (2021), <https://doi.org/10.1016/j.enbuild.2021.111418>.
- [13] R. Ade, M. Rehm, A summertime thermal analysis of New Zealand Homestar certified apartments for older people, *Build. Res. Inform.* 50 (2022), <https://doi.org/10.1080/09613218.2022.2038062>.
- [14] J. Zuo, S. Pullen, J. Palmer, H. Bennetts, N. Chileshe, T. Ma, Impacts of heat waves and corresponding measures: a review, *J. Clean Prod.* 92 (2015) 1–12, <https://doi.org/10.1016/J.JCLEPRO.2014.12.078>.
- [15] W. Plokker, J. Evers, C. Struck, A. Wijsman, J. Hensen, First experiences using climate scenarios for the netherlands in building performance simulation. IBPSA 2009 - International Building Performance Simulation Association, 2009, p. 2009.

- [16] D. Daly, P. Cooper, Z. Ma, Implications of global warming for commercial building retrofitting in Australian cities, *Build. Environ.* 74 (2014), <https://doi.org/10.1016/j.buildenv.2014.01.008>.
- [17] A practical guide to climate-resilient buildings & communities | UNEP - UN environment programme, <https://www.unep.org/resources/practical-guide-c-climate-resilient-buildings>.
- [18] S. Attia, R. Levinson, E. Ndongo, P. Holzer, O. Berk Kazanci, S. Homaei, C. Zhang, B.W. Olesen, D. Qi, M. Hamdy, P. Heiselberg, Resilient cooling of buildings to protect against heat waves and power outages: key concepts and definition, *Energy Build.* 239 (2021) 110869, <https://doi.org/10.1016/J.ENBUILD.2021.110869>.
- [19] C. Zhang, O.B. Kazanci, R. Levinson, P. Heiselberg, B.W. Olesen, G. Chiesa, B. Sodagar, Z. Ai, S. Selkowitz, M. Zinzi, A. Mahdavi, H. Teufel, M. Kolokotroni, A. Salvati, E. Bozonnet, F. Chtioui, P. Salagnac, R. Rahif, S. Attia, V. Lemort, E. Elnagar, H. Breesch, A. Sengupta, L.L. Wang, D. Qi, P. Stern, N. Yoon, D. I. Bogatu, R.F. Rupp, T. Arghand, S. Javed, J. Akander, A. Hayati, M. Cehlin, S. Sayadi, S. Forghani, H. Zhang, E. Arens, G. Zhang, Resilient cooling strategies – a critical review and qualitative assessment, *Energy Build.* 251 (2021) 111312, <https://doi.org/10.1016/J.ENBUILD.2021.111312>.
- [20] N. Yoon, W. Wu, Short-term thermal resilience and building energy flexibility using thermal mass and controlled natural ventilation, *Energy Build.* (2024) 114547, <https://doi.org/10.1016/J.ENBUILD.2024.114547>.
- [21] ASHRAE, ANSI/ASHRAE Standard 169-2013. Climatic Data for Building Design, ASHRAE, Atlanta, 2013.
- [22] N. Garrido, R. Capdevila, E. Tontodonati, L. Borghero, Numerical investigation of different cooling technologies during heatwaves in Catalan Mediterranean buildings, *J. Phys. Conf. Ser.* 2766 (2024) 012109, <https://doi.org/10.1088/1742-6596/2766/1/012109>.
- [23] L. Ji, C. Shu, A. Laouadi, M. Lacasse, L.(Leon) Wang, Quantifying improvement of building and zone level thermal resilience by cooling retrofits against summertime heat events, *Build. Environ.* 229 (2023) 109914, <https://doi.org/10.1016/J.BUILDENV.2022.109914>.
- [24] C. Zhang, O.B. Kazanci, S. Attia, R. Levinson, S.H. Lee, P. Holzer, A. Salvati, A. Machard, M. Pourabdollahtookaboni, A. Gaur, B.W. Olesen, P. Heiselberg, IEA EBC Annex 80 - dynamic simulation guideline for the performance testing of resilient cooling strategies, <https://vbn.aau.dk/en/publications/iea-ebc-annex-80-dynamic-simulation-guideline-for-the-performance>.
- [25] A.P. Gagge, J.A.J. Stolwijk, Y. Nishi, An effective temperature scale based on a simple model of human physiological regulatory response, *Memoirs Faculty Eng. Hokkaido Univ.* 13 (1972) 21–36.
- [26] M. Sheng, M. Reiner, K. Sun, T. Hong, Assessing thermal resilience of an assisted living facility during heat waves and cold snaps with power outages, *Build. Environ.* 230 (2023) 110001, <https://doi.org/10.1016/J.BUILDENV.2023.110001>.
- [27] R. Levinson, S.H. Lee, R. Levinson, S.H. Lee, Lawrence Berkeley National Laboratory LBL Publications title cool envelope benefits in future typical weather and heatwave conditions for single-family homes in Los Angeles, (2023). <https://doi.org/10.20357/B7DK61>.
- [28] J. Park, K.H. Lee, S.H. Lee, T. Hong, Benefits assessment of cool skin and ventilated cavity skin: saving energy and mitigating heat and grid stress, *Build. Environ.* 247 (2024) 111027.
- [29] A. Sengupta, M. Steeman, H. Breesch, Analysis of resilience of ventilative cooling technologies in a case study building, *ICRBE Procedia* (2020), <https://doi.org/10.32438/icrbe.202041>.
- [30] A. Sengupta, D. Al Assaad, J.B. Bastero, M. Steeman, H. Breesch, Impact of heatwaves and system shocks on a nearly zero energy educational building: is it resilient to overheating?, 234 (2023). <https://doi.org/10.1016/j.buildenv.2023.110152>.
- [31] A. Machard, A. Salvati, M.P. Tootkaboni, A. Gaur, J. Zou, L.L. Wang, F. Baba, H. Ge, F. Bre, E. Bozonnet, V. Corrado, X. Luo, R. Levinson, S.H. Lee, T. Hong, M. Salles Olinger, R.M. e. S. Machado, E.L.A. da Guarda, R.K. Veiga, R. Lamberts, A. Afshari, D. Ramon, H. Ngoc Dung Ngo, A. Sengupta, H. Breesch, N. Heijmans, J. Deltour, X. Kuborn, S. Sayadi, B. Qian, C. Zhang, R. Rahif, S. Attia, P. Stern, P. Holzer, Typical and extreme weather datasets for studying the resilience of buildings to climate change and heatwaves, *Sci. Data* 11 (2024) 1–21, <https://doi.org/10.1038/s41597-024-03319-8>, 2024 11:1.
- [32] A.F. Krelling, L.G. Eli, M.S. Olinger, R.M.E.S. Machado, A.P. Melo, R. Lamberts, A thermal performance standard for residential buildings in warm climates: lessons learned in Brazil, *Energy Build.* 281 (2023) 112770, <https://doi.org/10.1016/J.ENBUILD.2022.112770>.
- [33] M.A. Triana, R. Lamberts, P. Sassi, Characterisation of representative building typologies for social housing projects in Brazil and its energy performance, *Energy Policy* 87 (2015) 524–541, <https://doi.org/10.1016/J.ENPOL.2015.08.041>.
- [34] I. Ballarini, S.P. Corgnati, V. Corrado, Use of reference buildings to assess the energy saving potentials of the residential building stock: the experience of TABULA project, *Energy Policy* 68 (2014) 273–284, <https://doi.org/10.1016/J.ENPOL.2014.01.027>.
- [35] D. Al Assaad, A. Sengupta, H. Breesch, Demand-controlled ventilation in educational buildings: energy efficient but is it resilient? *Build. Environ.* 226 (2022) 109778 <https://doi.org/10.1016/J.BUILDENV.2022.109778>.
- [36] D. Al Assaad, A. Sengupta, H. Breesch, A novel quantitative assessment framework of the IAQ resilience performance of buildings: the resilience score metric, *Build. Environ.* 243 (2023), <https://doi.org/10.1016/j.buildenv.2023.110669>.
- [37] D. Amaripadath, M. Velickovic, S. Attia, Performance evaluation of a nearly zero-energy office building in temperate oceanic climate based on field measurements, *Energies* 15 (2022) 6755, <https://doi.org/10.3390/EN15186755>, 2022, Vol. 15, Page 6755.
- [38] D. Amaripadath, R. Paolini, D.J. Sailor, S. Attia, Comparative assessment of night ventilation performance in a nearly zero-energy office building during heat waves in Brussels, *J. Build. Eng.* 78 (2023) 107611, <https://doi.org/10.1016/J.JOBE.2023.107611>.
- [39] D. Amaripadath, R. Rahif, W. Zuo, M. Velickovic, C. Voglaire, S. Attia, Climate change sensitive sizing and design for nearly zero-energy office building systems in Brussels, *Energy Build.* 286 (2023) 112971, <https://doi.org/10.1016/J.ENBUILD.2023.112971>.
- [40] F.M. Baba, K.C.T. Cheong, H. Ge, R. Zmeureanu, L. Wang, D. Qi, Comparing overheating risk and mitigation strategies for two Canadian schools by using building simulation calibrated with measured data, *J. Build. Perform. Simul.* (2023), <https://doi.org/10.1080/19401493.2023.2290103>.
- [41] F.M. Baba, H. Ge, L.(Leon) Wang, R. Zmeureanu, Assessing and mitigating overheating risk in existing Canadian school buildings under extreme current and future climates, *Energy Build.* 279 (2023) 112710, <https://doi.org/10.1016/J.ENBUILD.2022.112710>.
- [42] F.M. Baba, H. Ge, R. Zmeureanu, L.(Leon) Wang, Optimizing overheating, lighting, and heating energy performances in Canadian school for climate change adaptation: sensitivity analysis and multi-objective optimization methodology, *Build. Environ.* 237 (2023) 110336, <https://doi.org/10.1016/J.BUILDENV.2023.110336>.
- [43] F.M. Baba, H. Ge, R. Zmeureanu, L.(Leon) Wang, Calibration of building model based on indoor temperature for overheating assessment using genetic algorithm: methodology, evaluation criteria, and case study, *Build. Environ.* 207 (2022) 108518, <https://doi.org/10.1016/J.BUILDENV.2021.108518>.
- [44] A. Machard, C. Inard, J.M. Alessandrini, C. Pelé, J. Ribéron, A methodology for assembling future weather files including heatwaves for building thermal simulations from the European coordinated regional downscaling experiment (EURO-CORDEX) climate data, *Energies* 13 (2020) 3424, <https://doi.org/10.3390/EN13133424>, 2020, Vol. 13, Page 3424.
- [45] P.H. Stone, J.S. Risbey, On the limitations of general circulation climate models, *Geophys. Res. Lett.* 17 (1990) 2173–2176, <https://doi.org/10.1029/GL0171012P02173>.
- [46] J. Younes, N. Ghaddar, K. Ghali, Impact assessment of climate change on naturally ventilated residential buildings in Lebanon—Overheating risk under future climate scenarios, in: *E3S Web of Conferences, EDP Sciences*, 2024, p. 07001.
- [47] D.S. Wilks, R.L. Wilby, The weather generation game: a review of stochastic weather models, *10.1177/030913339902300302* 23 (1999) 329–357. <https://doi.org/10.1177/030913339902300302>.
- [48] O. Lhotka, J. Kysely, E. Plavcova, Evaluation of major heat waves' mechanisms in EURO-CORDEX RCMs over Central Europe, *Clim. Dyn.* 50 (2018) 4249–4262, <https://doi.org/10.1007/S00382-017-3873-9/FIGURES/6>.
- [49] Cordex – Coordinated Regional Climate Downscaling Experiment, (n.d.). <https://cordex.org/> (accessed January 16, 2025).
- [50] AR5 Climate Change 2013: The physical science basis — IPCC, (n.d.). <https://www.ipcc.ch/report/ar5/wg1/> (accessed July 29, 2024).
- [51] D. Jacob, J. Petersen, B. Eggert, A. Alias, O.B. Christensen, L.M. Bouwer, A. Braun, A. Colette, M. Déqué, G. Georgievski, E. Georgopoulou, A. Gobiet, L. Menut, G. Nikulin, A. Haensler, N. Hempelmann, C. Jones, K. Keuler, S. Kovats, N. Kröner, S. Kotlarski, A. Kriegsmann, E. Martin, E. van Meijgaard, C. Moseley, S. Pfeifer, S. Preuschmann, C. Radermacher, K. Radtke, D. Rechid, M. Rounsevell, P. Samuelsson, S. Somot, J.F. Soussana, C. Teichmann, R. Valentini, R. Vautard, B. Weber, P. Yiou, EURO-CORDEX: new high-resolution climate change projections for European impact research, *Reg. Environ. Change* 14 (2014) 563–578, <https://doi.org/10.1007/S10113-013-0499-2/FIGURES/8>.
- [52] ISO 15927-4:2005 - performance hygrothermique des bâtiments — Calcul et présentation des données climatiques — Partie 4: données horaires pour l'évaluation du besoin énergétique annuel de chauffage et de refroidissement, (n. d.). <https://www.iso.org/fr/standard/41371.html> (accessed January 16, 2025).
- [53] G. Ouzeau, J.M. Soubeyroux, M. Schneider, R. Vautard, S. Planton, Heat waves analysis over France in present and future climate: application of a new method on the EURO-CORDEX ensemble, *Clim. Serv.* 4 (2016), <https://doi.org/10.1016/j.cliserv.2016.09.002>.
- [54] World Data Center for Climate, (n.d.). https://www.wdc-climate.de/ui/q?hierarchy_steps_ss=WDTF_Annex80_build_v1.0&entry_type_s=Dataset.
- [55] ASHRAE Standard 55 – Thermal environmental conditions for Human occupancy., <https://www.ashrae.org/technical-resources/bookstore/standard-55-thermal-environmental-conditions-for-human-occupancy>.
- [56] A.P. Gagge, J.A.J. Stolwijk, Y. Nishi, An effective temperature scale based on a simple model of human physiological regulatory response, *Memoirs Faculty Eng Hokkaido Univ.* 13 (1972) 21–36.
- [57] F. Tartarini, S. Schiavon, pythermalcomfort: a python package for thermal comfort research, *SoftwareX* 12 (2020) 100578, <https://doi.org/10.1016/j.softx.2020.100578>.
- [58] D.A. McIntyre, Indoor climate, (No Title) (1980).
- [59] W. Ji, Y. Zhu, B. Cao, Development of the predicted thermal sensation (PTS) model using the ASHRAE global thermal comfort database, *Energy Build.* 211 (2020) 109780, <https://doi.org/10.1016/J.ENBUILD.2020.109780>.
- [60] L. Ji, C. Shu, A. Laouadi, L. (Leon) Wang, M. Lacasse, Predicting older people's thermal sensation by a new integrated physiological-based and data-driven model, in: *INDOOR ENVIRONMENTAL QUALITY PERFORMANCE APPROACHES (IAQ 2020)*, PT 1, 2021.
- [61] J. Gao, Y. Wang, P. Wargocki, Comparative analysis of modified PMV models and SET models to predict human thermal sensation in naturally ventilated buildings, *Build. Environ.* 92 (2015), <https://doi.org/10.1016/j.buildenv.2015.04.030>.

- [62] A. Laouadi, M. Bartko, M.A. Lacasse, A new methodology of evaluation of overheating in buildings, *Energy Build.* 226 (2020), <https://doi.org/10.1016/j.enbuild.2020.110360>.
- [63] J. Xiong, Z. Lian, X. Zhou, J. You, Y. Lin, Effects of temperature steps on human health and thermal comfort, *Build. Environ.* 94 (2015) 144–154, <https://doi.org/10.1016/J.BUILDENV.2015.07.032>.
- [64] S. Hu, M. He, X. Zhang, H. Guan, P. Song, R. Liu, G. Liu, Cold and hot step-changes affecting thermal comfort and physiological indicators in winter, *Energy Build.* 254 (2022) 111587, <https://doi.org/10.1016/J.ENBUILD.2021.111587>.
- [65] A. Sengupta, D. Al Assaad, O. Berk Kazanci, J. Shinoda, H. Breesch, M. Steeman, Building and system design's impact on thermal resilience to overheating during heatwaves: an uncertainty and sensitivity analysis, *Build. Environ.* 265 (2024) 112031, <https://doi.org/10.1016/J.BUILDENV.2024.112031>.